ENERGY LEVELS IN LIGHT AND
MEDIUM WEIGHT NUCLEI

by

LCDR WILLIAM DAVID BAKER
and
LT JAY STANLEY HOWELL

COURSE VIII

ENERGY LEVELS IN LIGHT AND MEDIUM WEIGHT NUCLEI

by

Lieutenant Commander WILLIAM DAVID BAKER

S.B., U.S. Naval Academy
(1940)

and

Lieutenant JAY STANLEY HOWELL

S.B., U.S. Naval Academy
(1943)

SUBMITTED IN PARTIAL FULFILLMENT OF THE
REQUIREMENTS FOR THE DEGREE OF
MASTER OF SCIENCE IN PHYSICS

at the

MASSACHUSETTS INSTITUTE OF TECHNOLOGY
(1950)

TABLE OF CONTENTS

ACKNOWLEDGMENTS

The graduate study of Lieutenant Commander William D. Baker and Lieutenant Jay S. Howell at M.I.T. was sponsored by the United States Naval Postgraduate School and the Bureau of Ordnance, Navy Department. The work herein reported was undertaken under the Nuclear Shielding Project at M.I.T. which is sponsored by the Bureau of Ships and the Office of Naval Research under Navy Task Contract N5ori-07818.

The authors desire to express their deep appreciation to Dr. Clark Goodman for his guidance as thesis supervisor; to Dr. T.S. Gray and Mr. H.B. Frey for assistance in the design and construction of the electronics apparatus; and to Dr. W.M. Preston, Messrs. H. Willard and P. Stelson, and the many personnel of the Laboratory for Nuclear Science and Engineering who were so generous with their aid in conducting experiments at the Rockefeller Generator.

ACKNOWLEDGMENT

The graduate [illegible] Commander William E. [illegible] was sponsored by the [illegible] School and the Bureau of [illegible] Department. The work herein reported was [illegible] Nuclear Shielding Project at M.I.T., which is sponsored by the Bureau of Ships and the Office of Naval Research under Navy Task Contract N5ori-78-T.O.

The authors desire to express their deep appreciation to Mr. Clark Goodman for his guidance as thesis supervisor; to Dr. [illegible] Grey and Dr. [illegible] Frey for assistance in the design and construction of the electronics apparatus; and to Dr. [illegible] Trenholm, [illegible] and F. Stalson, and the many personnel of the Laboratory for Nuclear Science and Engineering who were so generous with their aid in conducting experiments at the Rockefeller Generator.

CHAPTER I

INTRODUCTION

By analogy with the development of spectroscopy, it is hoped that the accumulation of large quantities of information concerning the excited states of nuclei, such as level spacing, level width, angular momentum, and parity, may eventually lead to an understanding of nuclear forces and the development of a comprehensive theory of the nucleus. One of the most fundamental tools of nuclear investigation is the electrostatic generator, which has achieved its prominence by means of its flexibility of control of bombarding particle energy. The Rockefeller Generator at M.I.T., recently put into operation as a positive ion accelerator, will enable research to be conducted on elements which were previously unsuitable because of energy limitations. It is hoped that the results reported in this paper, among the first obtained with the Rockefeller Generator, will not only add to the store of nuclear information, but will also be useful in the evaluation of the performance of the generator.

Three elements were chosen for investigation: Li^7, Sc^{45}, and V^{51}. All three produce monoenergetic neut-

rons under proton bombardment*, hence make useful sources for use in the laboratory. The latter two are monoisotopic** in nature, and possess certain other advantages over Li^7 as neutron sources***. Actually, the results of our investigations indicate that the monochromaticity of the neutrons from the compound nuclei Ti^{46} and Cr^{52} is open to question, and must remain so until the disintegration scheme of the various levels found in the compound nuclei can be definitely established.

The characteristics of the $Li^7(p,n)$ reaction are well known for proton energies up to about 3 Mev. Our results have duplicated the known levels in the compound nucleus Be^8, and have established additional probable resonances at higher energies. In this same experiment we also confirmed the 0.48 Mev level in Li^7 by simple absorption of the gamma rays in lead. The position of the level was independently measured by coincidence absorption experiments using the procedure described by Rose (Ro 48). The fast amplifiers and coincidence circuit used in this measurement should prove useful for studying similar reactions in which a charged particle is emitted essentially simultaneously with a gamma ray from

---

* Recent evidence points to the existence of two neutron groups from a Li^7 target for $E_p > 2.31$ Mev. See Chapters VII and X. Cf. also (La 50), (Jo 50), and (Gr 50).

** Hess (He 49) has recently reported the isotope V^{50} to be present to one part in 400 in nature.

***See Chapter VIII.

the compound nucleus.

Our results for the medium weight nuclei, V^{51} and Sc^{45}, indicate the existence of many excited states. The observed level schemes have been compared with Wilson's spherical shell model of the nucleus (Wi 50), and are found to be in agreement with his hypothesis that energy levels with a constant spacing, independent of mass and excitation energy, exist in nuclei.

A rigorous quantitative test of Wilson's theory depends upon the use of mass values more accurate than those available at present. Using the best obtainable mass values, the agreement with observation is quite satisfactory, and in the case of Cr^{52}, striking. It must be recognized, however, that Wilson's theory is actually only an empirical fitting of observed data, and without further interpretation can lead one no further toward a fundamental understanding of the nucleus. Even so, his theory has several practical applications, which are discussed in Chapters VIII and X.

CHAPTER II

ELECTRONIC APPARATUS

Introduction

The past decade has witnessed a considerable development in pulse amplifiers, particularly for low-level signals of very short duration from electronic detectors of radiation. Fast amplifiers have been designed whose response approaches the limit attainable with conventional tubes and circuits. Eventually another factor of ten in speed of response may be achieved by the use of sub-miniature tubes and distributed parameter circuits. Beyond this apparently irreducible minimum, the limit is set by transit time of electrons.

Two fast amplifiers were constructed during an investigation of the possibility of measuring neutron energies in the resonance region (1 to 10^5 ev) by means of delayed coincidences, utilizing reactions in which gamma rays are emitted essentially simultaneously with the neutron. The energy resolution is given by $\frac{E}{dE} = \frac{t}{2\tau}$, where t is the time taken for the neutron to travel from source to detector, and 2τ is the time duration in the coincidence circuit within which the neutron and gamma pulses must fall if a coincidence output is to be recorded. A 10 kev neutron

travels a distance of one meter in 0.72 μ seconds. The energy resolution of the system for this neutron is thus $\frac{E}{\Delta E} = \frac{.36}{\tau}$ where τ is in μ seconds. To extend energy measurement beyond that attainable by the Columbia Velocity Selector (Ra 46), τ should be $\leqslant .05$. Accordingly, the system was constructed to conform to this figure as an upper limit. This selection requires detecting apparatus in which the time uncertainties, such as rise time and the delay between initial ionizing event and formation of output pulse, are $\leqslant .05$ μ seconds.

The Neutron Detector

The neutron detector presents the most difficulty. A boron (preferably B^{10}) impregnated phosphor used in conjunction with a photomultiplier tube would be ideal except that if thin enough to be transparent, its efficiency is too low, or if thick enough to achieve tolerable efficiency, it is opaque to its own fluorescence (Nu 49). An enriched boron trifluoride proportional counter is probably the next most logical choice. The general properties of such a counter are shown in Fig. 2-1a.

If the initial ionizing event is considered to be an impulse function, the output will be as shown. During the time (OA) required for the electron to travel from the point of initial ionization to within a few diameters of the center wire, essentially no output pulse appears. This time

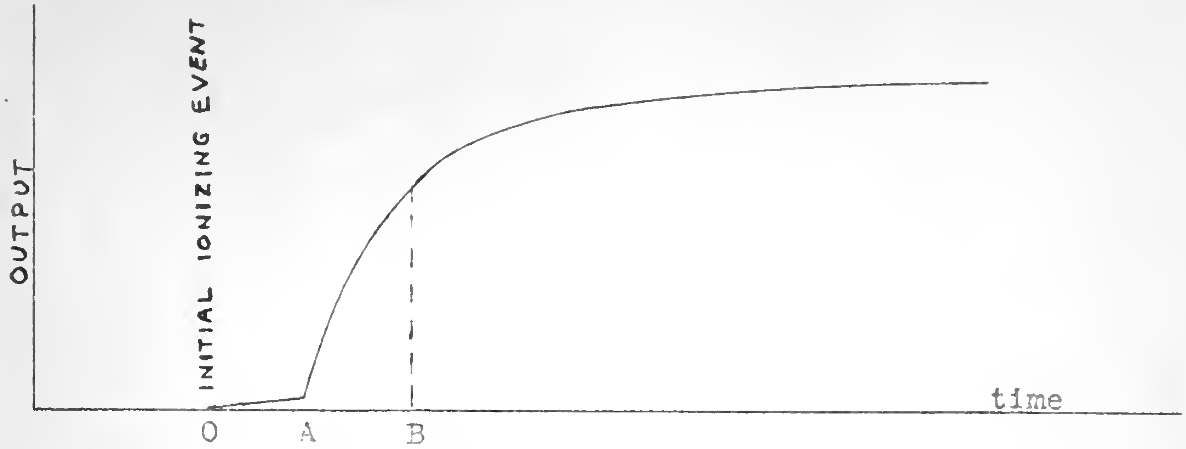

Fig. 2-1a. Current output of a BF_3 proportional counter.

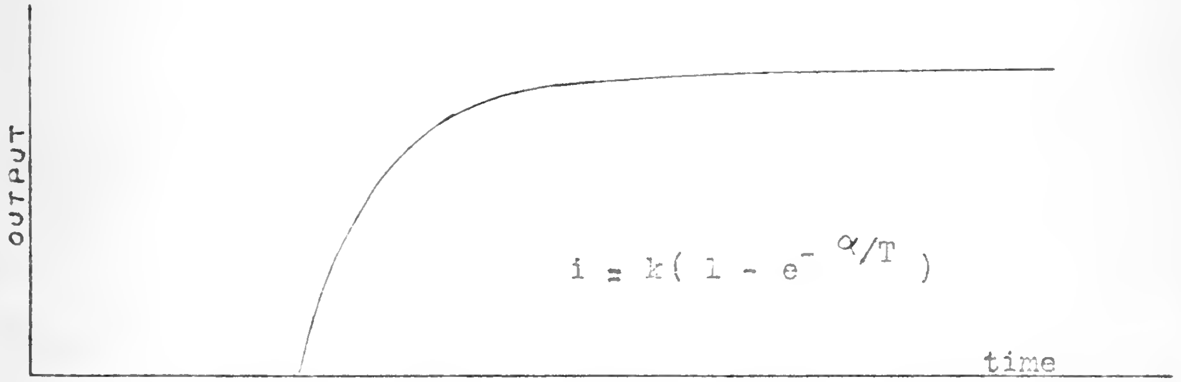

Fig. 2-1b. Form of output current from BF_3 counter assumed for analytical purposes.

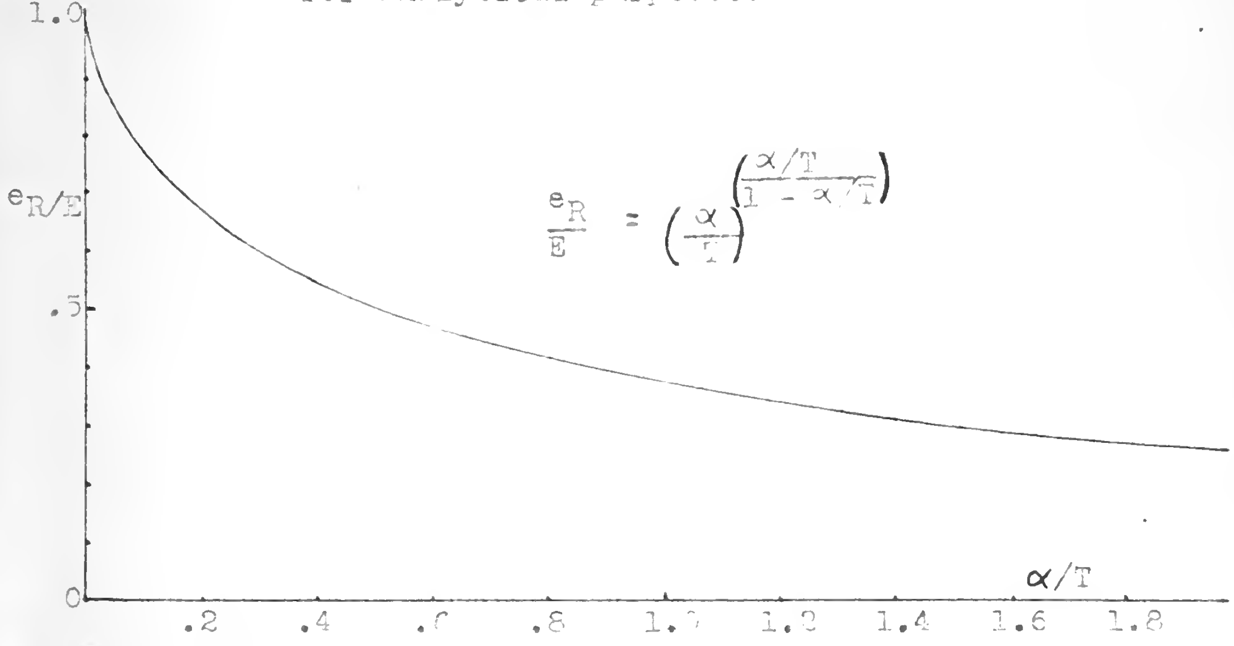

Fig. 2-1c.

can be computed using a curve given by Rossi and Staub (Ro 47). For voltages and pressures normally used ($E/p < 9 \frac{\text{volts}}{\text{cm-mmHg}}$) this curve can conveniently be represented by the linear relation: electron velocity $W = 10^7 E/p$. The resulting transit time will be too large by only a few percent. Thus for a typical boron counter: V = 2300 volts, p = 46 cmHg, anode radius 1.25 cm, and a 2 mil center wire:

$$W(r) = \frac{10^7}{460} \frac{2300}{r \, \ell n \, 166} \approx \frac{10^7}{r} ,$$

and the time required for an electron to travel from the counter wall to the center wire is:

$$T = \int_{1.25}^{0} \frac{r \, dr}{10^7} \approx 0.08 \, \mu \text{ seconds.}$$

When the electron avalanche approaches within a few diameters of the center wire, an output pulse with a rise time of about 10^{-7} seconds (AB in the figure) accompanies the electron collection. The remainder of the pulse is the result of positive ion collection and is of the order of 200 to 400 μ seconds. It is possible to measure the rise time by observing the pulse on a very fast oscilloscope. Such a method requires that the amplifier and oscilloscope be able to reproduce the pulse faithfully. The rise time may also be determined approximately by measuring the variation in pulse height as a function of the time constant of

a circuit which differentiates the pulse. (The parameter in this experiment was the output capacitor of the pre-amplifier, Fig. A-1.) The method assumes that the current pulse from a boron counter may be represented as $i = k(1 - e^{-t/\alpha})$, where α is the time required for the pulse to reach 63% of its final value. Using the Laplace transform, the voltage across the resistor of the differentiating circuit can be shown to be:

$$e_R = \frac{ET}{T - \alpha}\left[e^{-t/T} - e^{-t/\alpha}\right], \tag{2-1}$$

where $T = RC$, and E is the maximum value of e_R, obtained when $T \gg \alpha$. The maximum value of Eq. 2-1 is obtained by setting $de_R/dt = 0$:

$$e_R = \frac{ET}{T - \alpha}\left[e^{\frac{\alpha}{T-\alpha}\ln\frac{\alpha}{T}} - e^{\frac{T}{T-\alpha}\ln\frac{\alpha}{T}}\right] \tag{2-2}$$

which reduces to

$$e_R = E\, x^{\frac{x}{1-x}}, \quad x = \alpha/T . \tag{2-3}$$

The dimensionless plot of e_R/E versus α/T is shown in Fig. 2-1c. The experimentally observed values of e_R/E are then entered as ordinate, and the corresponding values of α/T used to compute α, as indicated in Table 2-1.

TABLE 2-1

Pulse Height	Capacitor in $\mu\mu f$	e_R/E	α/T	α in μ sec.
50.0 volts	4985	1.	~0	indef.
50.0	3040	1.	~0	indef.
44.0	1380	.88	.037	.051
42.8	1102	.856	.050	.055
41.9	1025	.839	.059	.061
41.1	914	.823	.066	.061
40.3	813	.806	.075	.061
38.0	727	.760	.110	.080
34.6	633	.692	.170	.108
30.6	513	.613	.272	.140
27.2	432	.545	.398	.172
22.1	332	.442	.670	.222
15.5	219	.310	1.40	.306
10.7	114	.214	2.50	.286

Average α = 0.133 μ sec.

The fact that the observed values for α are not nearly the same is caused by:

a. The output pulse cannot truly be represented by the analytical function assumed.

b. Errors may exist in the measurement of capacitors used.

c. Determination of the pulse height is subject to an error of about 10%.

d. Not all pulses from a given counter will have the same shape as indicated in Fig. 2-1a. The transit time (OA), the electron collection time (AB), and the pulse height are functions of the location in the counter of the initial ionizing event, and the direction in which the ionizing particle travels. Subject to these conditions, the rise time and transit time may vary by as much as a factor of three with the values quoted in preceding paragraphs.

However, since no single value of α differs radically from the average, it is felt that the method provides a fairly reliable yet easy means of estimating very fast rise times.

The use of a 100 $\mu\mu f$ capacitor in the preamplifier output requires a sacrifice of a factor of 5 in voltage gain. However, it is considered best to secure the necessary gain by additional amplification, thereby retaining the small differentiating time constant ($100 \times 1000 \times 10^{-12} = 10^{-7}$ sec.) in order to prevent the pile up of pulses at fast counting rates (i.e., greater than about 500,000 sec^{-1}).

The Gamma Ray Detector

As mentioned previously, the scintillation counter makes an ideal detector for many purposes. Its rise time and pulse duration are very short. The photomultiplier tube may be directly connected to the preamplifier, eliminating undesirable cable capacitances. Its efficiency for gamma ray detection may be made as high as 15% by choice of a thick, clear anthracene crystal.

Sketches analogous to Fig. 2-1a may be drawn for the scintillation counter as shown in Fig. 2-2a, b. As before, let the initial ionizing event be represented by an impulse function. Dependent upon dynode voltage, dynode spacing, and number of dynodes, no output will appear on the collector electrode for about 4×10^{-9} seconds (OA), following activation of the photosensitive surface by a

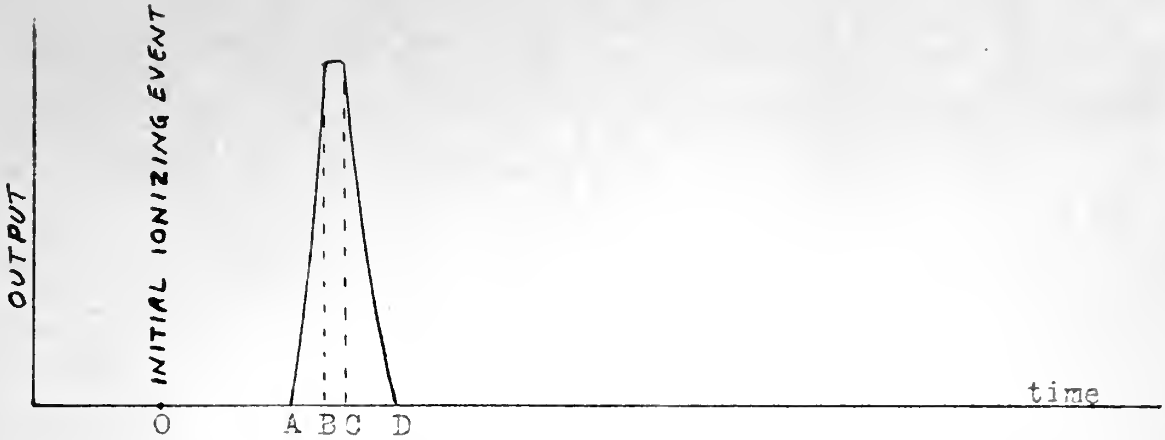

Fig. 2-2a. The current output pulse of a photomultiplier if the photocathode is directly activated by radiation.

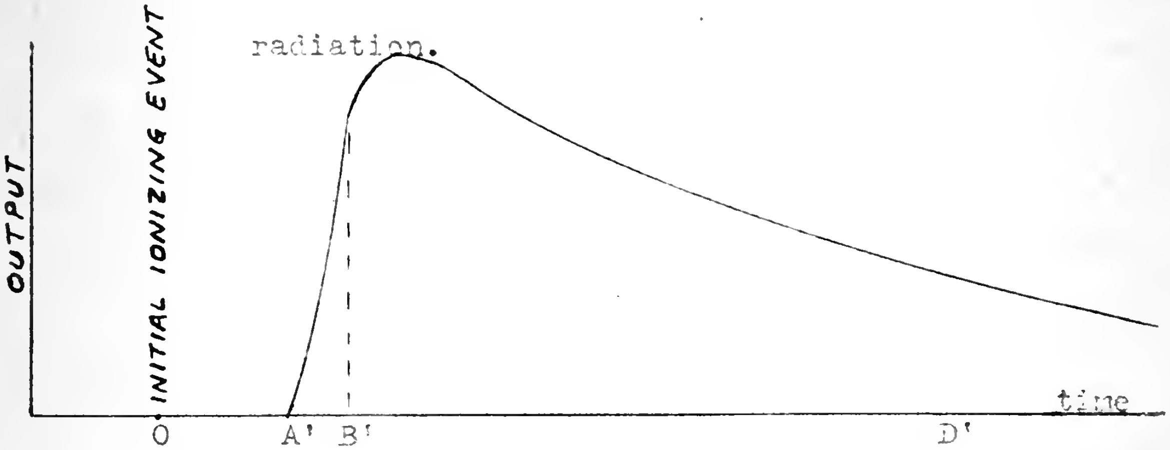

Fig. 2-2b. The current output pulse of a photomultiplier if the photocathode is activated by radiation from a luminescent crystal or phosphor.

photon. The pulse has a rise time of about 6 x 10^{-10} seconds (AB) followed by a comparatively constant output for about 3 x 10^{-10} seconds (BC) which represents the variation in time required for different electrons to travel through the tube (De 48, Ow 44). The pulse has a decay time (CD) approximately equal to its rise time.

When a crystal or phosphor is placed before the photosensitive surface, the output pulse assumes more nearly the shape of the light pulse in the crystal, as indicated in Fig. 2-2b. The electron transit time, 4 x 10^{-9} seconds (OA'), remains. However, the pulse now has a rise time (A'B') which is characteristic of the crystal. Similarly, the pulse has a decay time (B'D') also characteristic of the crystal. The rise time of most crystals has been found to be about 2 x 10^{-9} seconds (Co 48, Or 49); but the decay time varies between wide limits. Some of the faster decay times have been given by Collins (Co 48) as:

Naphthalene - 5.7 x 10^{-8} sec.
Anthracene - 1.3 x 10^{-8} sec.
Penanthrene - 0.9 x 10^{-8} sec.

These figures are to be contrasted with the somewhat slower decay times of inorganic phosphors (Jo 49) such as:

ZnS (Ag) - 1 x 10^{-5} seconds
CdS (Ag) - 1 x 10^{-4} seconds

The choice of crystal or phosphor depends upon (1) speed, (2) efficiency, and (3) pulse height. Inorganic crystals and phosphors have larger pulse heights and greater efficiencies but less speed than organic. In general the emission time of inorganic phosphors is $> 10^{-7}$ seconds, the emission time of organic phosphors $< 10^{-7}$ seconds. The increased use of scintillation counters has caused the investigation of the properties of many crystals and phosphors (Co 48, Or 49, Jo 49, Ho 49, Ga 49, Le 44, Mo 48, Ho 48, and many others).

The best available crystal was a cylinder of anthracene, 1.15 mm. thick, with an irregularly shaped base roughly 13 cm^2 in area. The photomultiplier tube (RCA 5819), surrounded by a mu-metal shield, was enclosed in a light tight brass box, and mounted integrally with its preamplifier.

Since the apparatus was to be used in the vicinity of the magnet at the Rockefeller generator, it was necessary to test the effect, if any, of the stray magnetic field on the operation of the photomultiplier tube. This was done using a 10 μ curie radium gamma source, with the counter about 1 meter distant from the magnet. The results appear in Table 2-2.

TABLE 2-2

Magnetometer Setting	Counts in 4 Minutes	$x - \bar{x}$	$(x - \bar{x})^2$
0	67132	-314	98600
1.5	67476	30	900
3.0	67828	382	146000
4.5	67779	333	111000
6.0	67480	34	1160
9.0	67323	-123	15200
12.0	67119	-327	106800
15.0	66985	-461	213000
	$\bar{x} = 67446$		$\mathcal{E} = 692660$

$$\chi^2 = 692660/67446 = 10.3$$

$F = (8-1) = 7$ degrees of freedom, and therefore $P = 0.2$, is the probability that a repetition of the experiment would show greater deviations from the expected value. Since the counting rate shows no trend with magnetometer setting, and since the probability P is such as to indicate that the data satisfy the randomicity test, it has been concluded that the stray magnetic field has no measurable effect upon the operation of the scintillation counter under the conditions indicated.

Preamplifiers

The preamplifiers for the neutron and gamma ray detectors are essentially identical. They are cathode followers, with a physical layout designed to give the best possible rise time. When tested alone using a pulse generator input, each showeda rise time of less than 0.01 μ

second. Type RG 65 U delay line of characteristic impedance 1000 ohms connects each preamplifier to its appropriate amplifier. This delay line together with the output capacitor of the preamplifier serves as a differentiating circuit so that "pile up" of pulses will not occur in later stages of the circuit. From the circuit diagrams of the preamplifiers, Fig. A-1 and A-2, it is seen that the differentiating time constant is $100 \times 1000 \times 10^{-12} = 10^{-7}$ seconds in the case of the scintillation counter preamplifier and $500 \times 1000 \times 10^{-12} = 5 \times 10^{-7}$ seconds in the case of the boron counter preamplifier. Thus average counting rates from random pulses of roughly 10^6 sec^{-1} and 5×10^5 sec^{-1} respectively will not result in serious pile up.

Delay line was chosen as the connection between preamplifiers and amplifiers for the following reasons: (1) delayed coincidence methods can be used simply by inserting extra lengths of delay line in one channel or the other; (2) the value of the characteristic impedance of the delay line is convenient for use in the differentiating circuit, as explained above; and (3) it is more convenient to drive the delay line at this (low level) point in the circuit rather than between the amplifier and coincidence circuit, since if the delay line is at the latter point, one must use an amplifier output tube capable of supplying enough current to produce an output pulse across the delay line sufficient to insure that the coincidence tube is completely cut off.

The Amplifiers

Except for slight modifications, the amplifiers follow an original design of Elmore, who has presented the problems arising in fast pulse amplifier design (El 48), as well as an analysis of these circuits (El 48a).

The theoretical analysis of fast pulse amplifiers is most easily accomplished by means of the Laplace transform, since this mathematical tool lends itself well to the pulse shapes experienced. The method is applicable only if the response of the system to a unit step function shows a monotonic rise. Since oscillations are undesirable in pulse amplifiers for particle counting, this is no deterrent to use of the method.

Let e'(t) be the response of the system to a unit impulse function. Then, in order to approach the problem analytically the following definitions are made: the delay time T_D is the time to the centroid of e'(t); i.e.,

$$T_D = \int_0^{\infty} t\, e'(t)dt,$$

and the rise time T_R is proportional to the radius of gyration of the area of e'(t); i.e.,

$$T_R = \left\{ 2\pi \left[\int_0^{\infty} t^2 e'(t)dt - T_D{}^2 \right] \right\}^{1/2},$$

where $(2\pi)^{1/2}$ is a constant of proportionality arising from the fact that e'(t) from an n stage amplifier approaches more and more closely a Normal Law distribution curve

("Gaussian" error curve) with increasing n. Fig. 2-3 shows graphically the definitions of T_R and T_D.

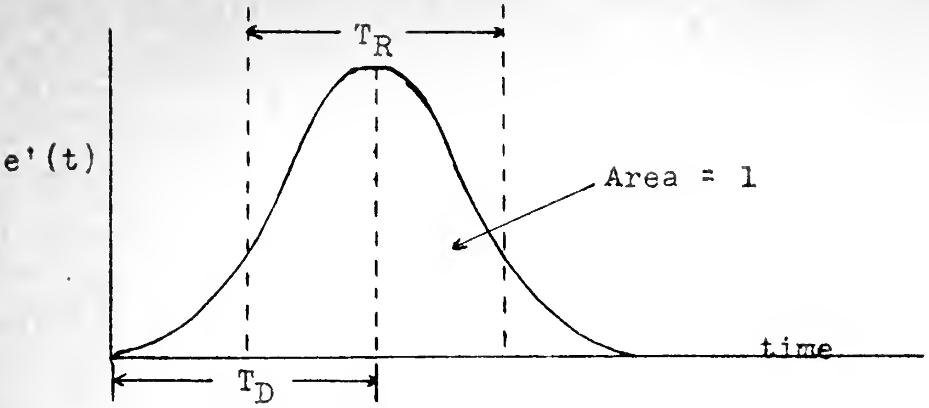

Fig. 2-3a. T_R and T_D as defined in the text.

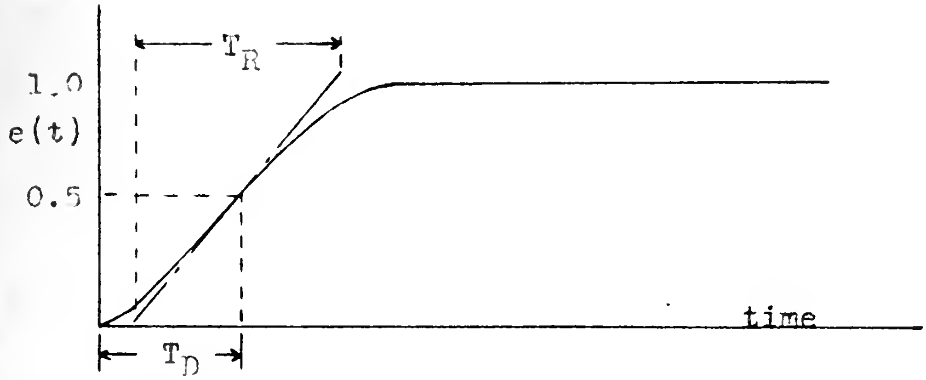

Fig. 2-3b. T_R and T_D as usually defined in the laboratory. The two systems of definition yield essentially the same numerical result. That of Fig. 2-3a lends itself well to mathematical analysis.

As a consequence of these definitions, the system function g(s) and the transient response e'(t) are related directly by the Laplace transform,

$$g(s) = \int_0^{\infty} e'(t)\, e^{-st}\, dt \quad ,$$

where s is the complex angular frequency, $\sigma + j\omega$.

The practical importance of the analysis is that it indicates that for minimum rise time the poles of $g(s)$ must indeed be a single multiple order pole situated on the negative real axis of the s-plane (for a monotonic response), and hence that each stage must be compensated so that this situation will exist.

The rise time T for an n stage amplifier of overall gain G, whose individual stages are properly compensated to give the same rise time T_o, is

$$T = \sqrt{n}\, T_o$$

$$= \left[\prod_{1}^{n} \mathcal{T}_i\right]^{1/n} \sqrt{n}\, G^{1/n} \qquad (2\text{-}4)$$

where $\mathcal{T}$ is a figure-of-merit for an interstage network and is numerically equal to $\frac{\sqrt{2\pi}C}{S\,Gm}$, where C is the sum of parasitic capacitances of the stage, Gm is the tube transconductance, and S is a numerical factor (from 1 to about 2.5) obtained from the Laplace transform of the system function for a given stage. If the $\mathcal{T}_i$ are made equal by proper choice of plate resistors and compensating inductance, then $T = \mathcal{T}_o \sqrt{n}\, G^{1/n}$. Thus the overall rise time has a minimum for

$$n = 2 \ln G$$

$$n = 2 \ln G_o^{\,n}$$

$$\text{or} \quad G_o = e^{1/2} = 1.65 \text{ per stage.}$$

Such a low gain per stage requirement for minimum rise time

makes excessive the number of stages required for amplifying signals from particle detectors. Fortunately, Eq. 2-4 has a broad minimum, so that the gain per stage may be raised to 2.7, with only a 10% increase in the rise time. In the amplifiers constructed for this work, a gain per stage of 3 was used, giving an overall gain of $3^6 = 740$. The rise time, for a step-function input was observed to be 0.05 microseconds.

The method of compensating was accomplished by a four terminal network, and is indicated schematically in Fig. 2-4.

An increase by a factor of 3 in overall gain was achieved over Elmore's original design by adding a stage identical with the first directly in front of it. This increase in gain coupled with the fact that the compensating network gives pulses about a 1% overshoot, combined to make the problem of pulse overshoots troublesome. However, the difficulty was effectively eliminated by insertion of series diodes (Type IN34 crystals) in the grid circuit of the Type 807 tube.

The amplifier has both a positive and negative output, the former being led to a scaler for obtaining the single counting rate, the latter being led to one channel of a coincidence circuit. The schematic diagram of the amplifier is shown in Fig. A-3.

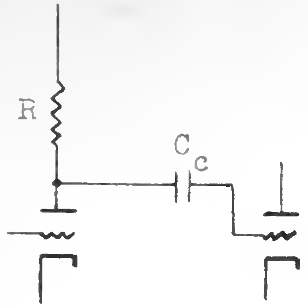

Fig. 2-4a.

Uncompensated network.

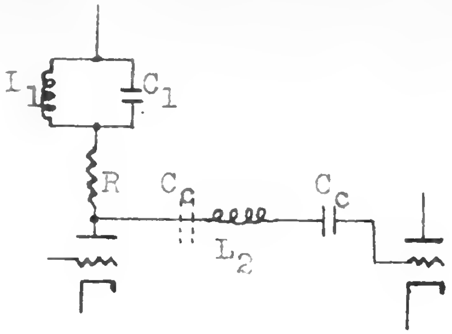

Fig. 2-4b.

Compensated network.

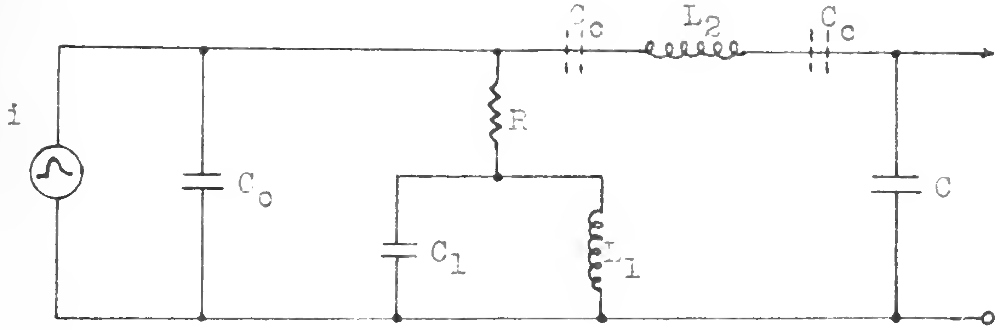

Fig. 2-4c. Equivalent circuit for the compensated network when the output capacitance of one tube is one half the input capacitance of the following stage. The coupling capacitor C_c may be shifted as indicated by the dotted lines to make the ratio of output to input capacitance equal to one half.

$C_c = 0.5C$, $C_1 = 0.22C$, $L_1 = 0.2R^2C$, $L_2 = 0.7R^2C$

The Coincidence Circuit

The coincidence circuit has been developed from a design proposed by Bell (Be 49), and consists basically of two tubes with a common plate supply voltage delivered through a section of delay line which serves as a pulse forming device.

Each input is constructed with a type IN44 Western Electric (low capacitance) crystal diode which is so oriented as to reject positive overshoots on pulses from the amplifiers. The diodes serve an additional purpose in that an adjustable bias may be applied across them so that they act to discriminate against pulses whose height is less than a given value.

The pulses developed across the delay line in the plate circuit of the coincidence tubes are fed to a discriminating stage which, when biased negatively, produces an output pulse only when both coincidence tubes are cut off within a time equal to the double delay time of the delay line used as the pulse former. However, operation of this stage at such a large negative bias necessarily means that the tube is in the region of low transconductance; hence a stage of amplification is required following this discriminator. From the amplifying stage, the pulses are fed into a cathode follower designed to drive the coaxial cable to the scaling circuit.

The effect of various lengths of delay line in

the plate circuit of the coincidence tubes was tested by applying the same signal to both inputs through various lengths of delay line, and measuring the coincidence rate as a function of the difference in length of delay line between signal source and the two inputs. The results are shown in Fig. 2-5a for two different lengths of pulse forming delay line. The simple expedient of changing the length of the pulse-forming delay line enables one to choose the resolution time of the apparatus, that is, the time within which pulses from the single channels must appear at the coincidence circuit input in order that a coincidence be registered.

The resolution time can also be varied by changing the bias on the discriminating stage, since the pulses possess a finite rise and decay time. Thus, as the negative bias is increased, only the more narrow tops of the pulses are effective in causing the discriminating stage to conduct, and one obtains a shorter resolution time. This effect is shown in Fig. 2-5b.

Ideally, it is desirable for coincidence pulses to have the same rise time and an amplitude several times larger than that required to cut off the coincidence tube. It is quite difficult to achieve these features, since both the boron counter and scintillation counter have large variations in output pulse height as well as significant variations in pulse rise time. The effects of these variations

have been reduced by amplifying the counter pulses so that the maximum input pulses to the coincidence tube grids have a height of about 60 volts. Even so, some of the smaller pulses have amplitudes less than 6.7 volts, which is just sufficient to cut off the coincidence tubes. However, the great majority of signal pulses are clipped so that the output of the coincidence circuit consists largely of pulses of equal height, although a few of smaller height are present. The integral bias curves, Fig. 2-5c, demonstrate the action of the coincidence circuit in reducing nearly all pulses to a uniform height.

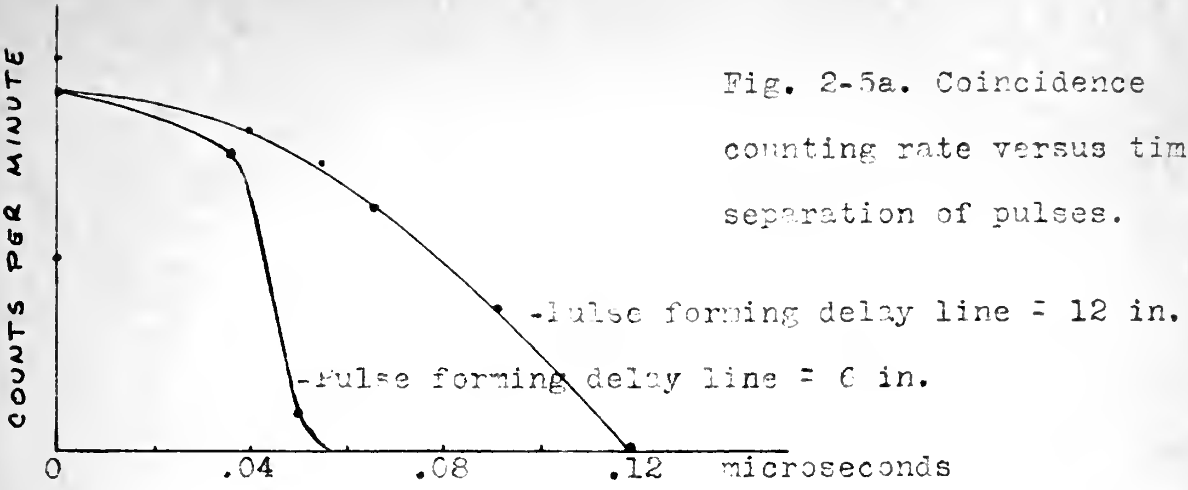

Fig. 2-5a. Coincidence counting rate versus time separation of pulses.

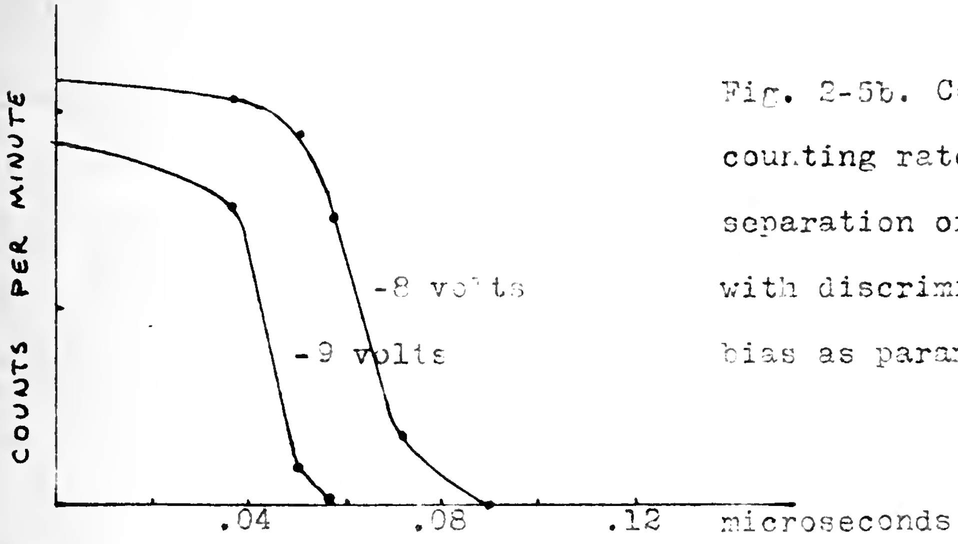

Fig. 2-5b. Coincidence counting rate versus time separation of pulses, with discriminator tube bias as parameter.

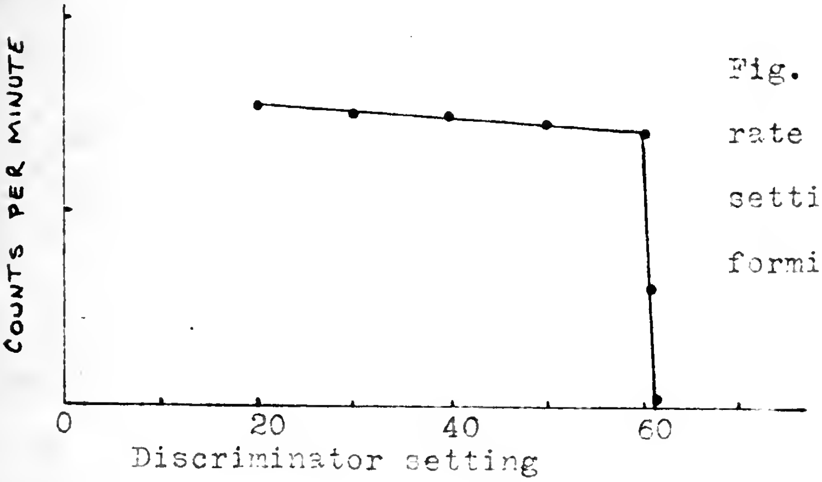

Fig. 2-5c. Scaler counting rate versus discriminator setting, indicating uniformity of pulse height.

CHAPTER III

AN ANALYSIS OF THE TIME-OF-FLIGHT METHOD FOR DETERMINING RESONANCE NEUTRON ENERGIES

The possibility of measuring the time-of-flight of neutrons for energies up to about 100 kev was proposed as an experiment which might be performed with the electronic equipment described in the previous chapter. Specifically, the proposal was to measure the low energy end of the neutron spectrum emitted by a Po-Be or Ra-Be source. With the source next to the scintillation counter and about one meter from the neutron detector, n-γ coincidences would be observed as a function of delay inserted in the γ-channel. With corrections for random coincidences and for the variation of detector efficiencies with energy, this measurement would give the distribution of neutron energies. Since a 100 kev neutron requires 0.227 microseconds to travel 1 meter, and since this time is considerably greater than the resolving time of the equipment, it would appear that fairly good energy resolution might be obtained for energies up to about 100 kev.

Before proceeding with the experiment, it was necessary to estimate the counting periods which would be required if reasonable statistical accuracy were to be

obtained. To this end, an assumption about the probable character of the spectrum being investigated must be made. Dacey and Paine (Da 49) give a summary of work on the neutron spectra from Ra-Be and Po-Be sources. They include an analysis of the energetics of the $Be^9(\alpha,n)C^{12}$ reaction, and they show that neutrons of energies less than 0.7 Mev are unlikely to be produced in the reaction. To account for lower energies, the following sequence has been suggested (Bj 38):

$$Be^9 + He^4 \longrightarrow C^{13*} \longrightarrow Be^{9*} + He^4$$
$$Be^{9*} \longrightarrow Be^8 + n$$

or, more likely,

$$Be^{9*} \longrightarrow 2\ He^4 + n$$

The overall Q-values are -1.63 Mev and -1.74 Mev. The Be^{9*} nucleus may have quite a range of velocities at the moment the neutron is emitted. The neutrons, therefore, will have a considerable spread in energy, and will include some with very low energies in the laboratory coordinates. Measurements of the Ra-Be neutron spectrum (De 45) and the Po-Be spectrum (Pe --) are cited by Dacey and Paine. No measurements below 100 kev are shown, but the trend of the curves suggests that the number of neutrons decreases with decreasing energy. Yalow and coworkers (Ya 46) have estimated that $\lesssim$ 10 per cent of the neutrons from a Ra-Be source have energies less than 100

kev. On the basis of the foregoing information, the assumption was made that 10% of the neutrons from the source have energies less than 100 kev and that the distribution is such that the number of neutrons of a given energy is proportional to that energy. Diagrammatically, the assumption is the following:

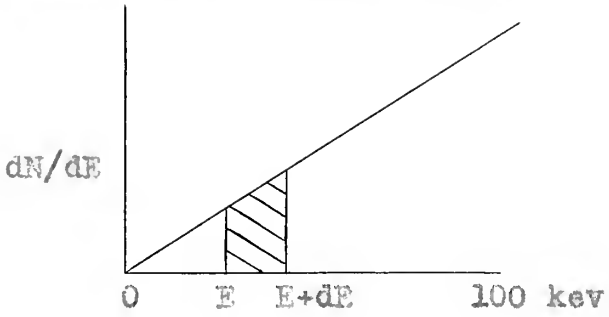

N_t = total number of neutrons from the source.

$$\int_0^{100} (dN/dE)\,dE = N_t/10$$

$$dN/dE = kE = (N_t/5 \times 10^4)E \qquad (3\text{-}1)$$

With this assumption, an analysis of the expected counting times was carried out. The method and much of the notation in what follows are due to Dunworth (Du 40). All units are c.g.s. except that energies are expressed in kev.

The time-of-flight t of a neutron of energy E over a distance d_2 between the source and the neutron detector will be

$$t = d_2(m/2E)^{1/2} = 2.27 \times 10^{-8}\, d_2/E^{1/2} \qquad (3\text{-}2)$$

The coincidence circuit has a finite resolving time τ and therefore there is a range dE over which the neutron ener-

gy may vary and yet cause a true coincidence to be recorded. This range is given by

$$dE = (2\tau/t)E \qquad (3\text{-}3)$$

The number of neutrons dN whose energies lie within this range is obtained by combining (3-1), (3-2), and (3-3):

$$dN = (N_t E^{5/2} \tau)/(5.6 \times 10^{-4}\ d_2)$$

These neutrons will be detected with a net efficiency (including solid angle) e_2, and their accompanying γ-rays will be detected with a net efficiency e_1. The expected genuine coincidence rate G is then

$$G = dN \cdot e_1 \cdot e_2$$

All the neutrons and γ-rays emitted by the source will contribute to the false coincidence rate F. The detection efficiencies will be averages for the entire spectrum. Hence

$$F = 2\ N_t^2 \cdot e_{1(av)} \cdot e_{2(av)}$$

C, the coincidence rate due to cosmic particles, will be taken as negligible. Dunworth shows that the total time of counting T which is required to attain a given fractional standard deviation f in the genuine rate G is

$$T = \frac{G + F}{f^2}\ \frac{1}{G^2}$$

provided the error in determining F is small. Substituting for F and G from the equations above gives

$$T = \frac{31.4\text{x}10^{-8}\ d_2^2\left[(E^{5/2}/5.6\text{x}10^{-4}\ d_2)e_1e_2 + 2N_t\ e_{1(av)}e_{2(av)}\right]}{N_t\ F^5\ \mathcal{T}\ f^2(e_1e_2)^2}$$

In order to estimate the counting times to be expected, the following numerical values were substituted in this equation:

$d_2 = 100$ cm. $\quad e_1 = 3.5 \times 10^{-2}$
$\mathcal{T} = 10^{-7}$ sec. $\quad e_2 = 1.3 \times 10^{-7}$
$E = 25$ kev $\quad e_{1(av)} = 3.5 \times 10^{-2}$
$f = 10\%$ $\quad e_{2(av)} = 4.2 \times 10^{-8}$

The values in the left-hand column were selected to give reasonable accuracy and resolution. The efficiencies are based on measurements using a Po-Be source of known strength, except for e_2 which was computed from the known characteristics of the BF_3 counter. The source strength N_t available was about 2×10^5 neutrons per second. The result of the calculation is

$$T \approx 800 \text{ days.}$$

With an optimum source, one in which $N_t = 1/2\mathcal{T}$, this figure would be about 600 days.

Since T represents the counting time required to to establish one point on the distribution curve, and since the assumptions upon which these values are based

seem optimistic, it appears that measurements of this kind must await the development of more efficient neutron detectors.

CHAPTER IV

THE ROCKEFELLER GENERATOR

The measurements described in later chapters were made at the Rockefeller Generator, which has recently been put into operation as a positive ion accelerator. A proton or deuteron beam is accelerated vertically from the ion source in the terminal through an 8-foot tube into a deflection chamber where it is bent to a horizontal direction by an analyzing magnet. The beam strikes the target at a height of 102 cm. from the concrete floor and 230 cm. from the nearest walls, also of concrete. A pressure of about 15 mμ Hg in the tube and chamber gives a well-defined beam of about 2 μ amp of H^+ or D^+.

At present the energy of the beam striking the target is controlled by manual adjustment of the current through the analyzing magnet. In the near future, a method of automatic beam energy control will be available. This method will employ a magnet flux regulator which receives its error signal from the deviations from the nuclear magnetic resonance condition of protons in a hydrogenous liquid. The error signal is obtained from a pick-up coil in which a voltage is generated by nuclear induction (Bl 46, 46a,b, To 49, Em 49). This method of

energy control, coupled with adjustment of the entrance and exit slits of the analyzing magnet, will permit an energy resolution of about 0.01%. The present energy resolution of 0.1% is sufficient for many preliminary and exploratory experiments such as are described in this paper.

The calibration of the generating voltmeter, whose readings determine the beam energy, is based on the $H^3(p,n)$, $Li^7(p,n)$, and $C^{13}(p,n)$ reactions which have sharp, well-determined thresholds for neutron production. The Li^7 reaction gave points at 1.881 and 3.762 Mev, the latter using H_2^+. The calibration points obtained were:

Generating Voltmeter	Energy of Beam (Mev)
22.0	0.986 (Ta 49)
40.5	1.881 (Sh 49)
70.8	3.236 (Sm 50)
82.0	3.762

The plot of beam energy versus generating voltmeter setting, Fig. 4-1, is not quite linear. More calibration points are needed to determine precisely the extent of the non-linearity, particularly at the lower voltmeter settings.

To date, no extensive study has been made of background as a function of beam energy and location in the target room. A rough estimate of the background was obtained using a piece of clean tantalum, which serves

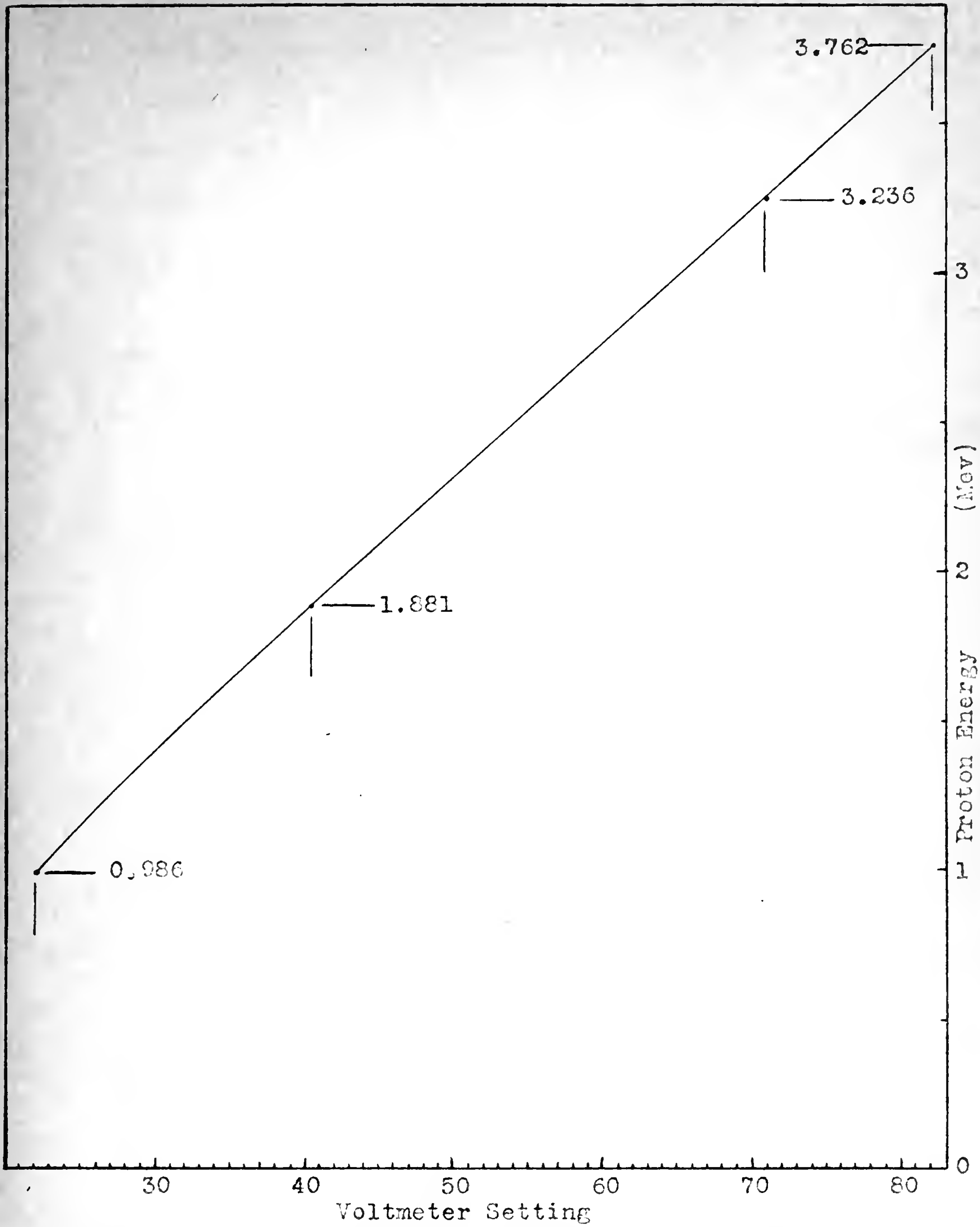

Fig. 4-1. Calibration curve for the Rockefeller Generator.

as a backing for most targets. The neutron and gamma ray counting rates were observed as a function of proton beam energy. The tantalum is mill quality, unannealed. It was obtained from the Fansteel Metallurgical Corporation of Hartford, Connecticut, which specifies its content as:

Tantalum - 99.9%
Iron - 0.03%
Carbon - 0.03%

The neutron and gamma ray yield curves from this target are shown in Figs. 4-2 and 4-3. The rise in neutron counting rate at a generating voltmeter setting of 71 is believed to be the effect of the carbon impurity of the tantalum, plus the effects of carbon from grease in the vacuum system, which may collect on the slits or be deposited on the target during bombardment. Thus Figs. 4-2 and 4-3 indicate the extent of undesirable neutron and gamma radiation from the tantalum target backing and various parts of the generator which the beam may strike. A comparison of these figures with the yield curves of later chapters shows that in general, the counting rates plotted on Figs. 4-2 and 4-3 are negligible compared to the counting rates observed with the targets studied. In a few isolated instances, for example in determining the $V^{51}(p,n)Cr^{51}$ threshold, it was necessary to consider this background.

The question of background has been troublesome

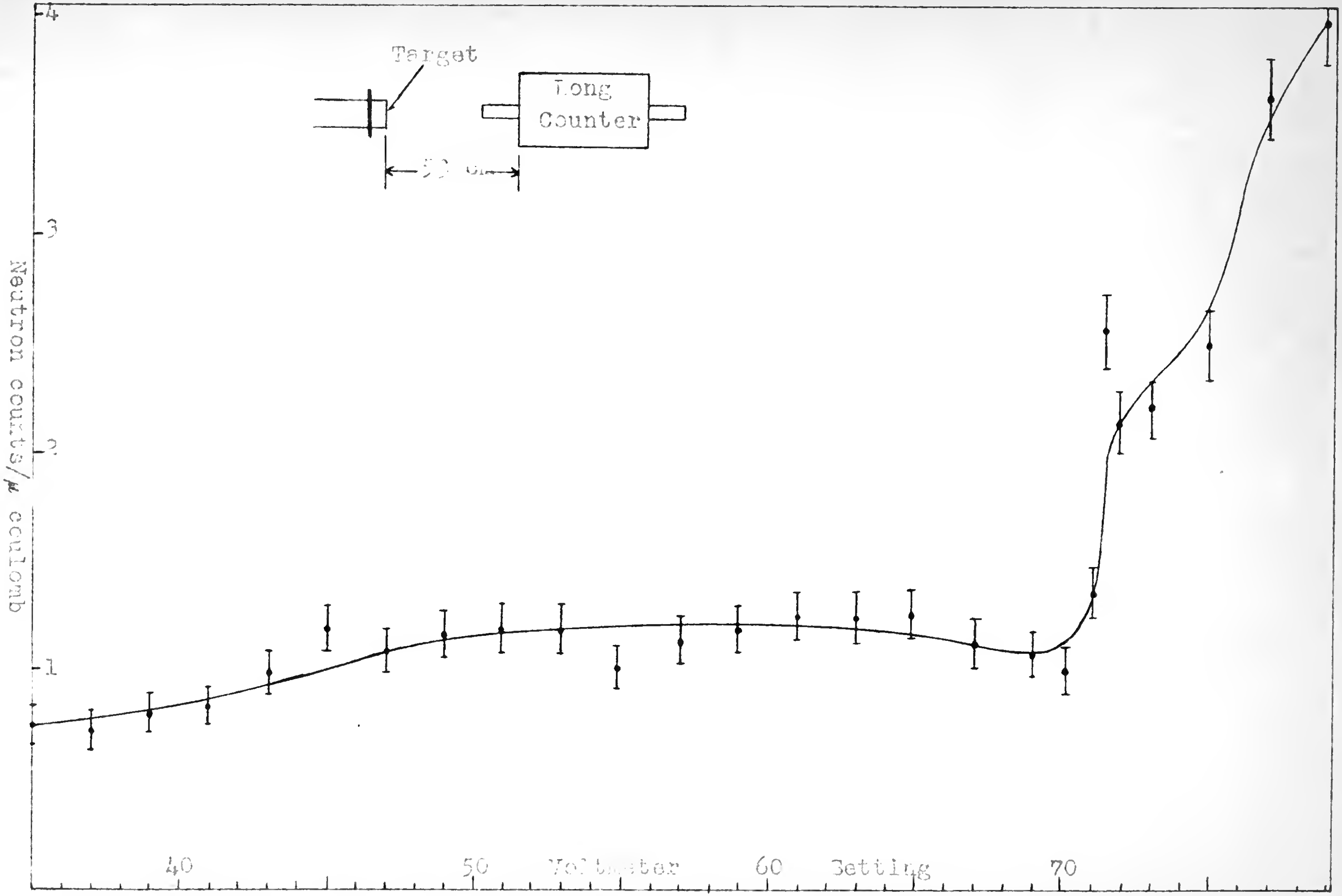

Fig. 4-2. Neutron yield from a Ta target bombarded by protons.

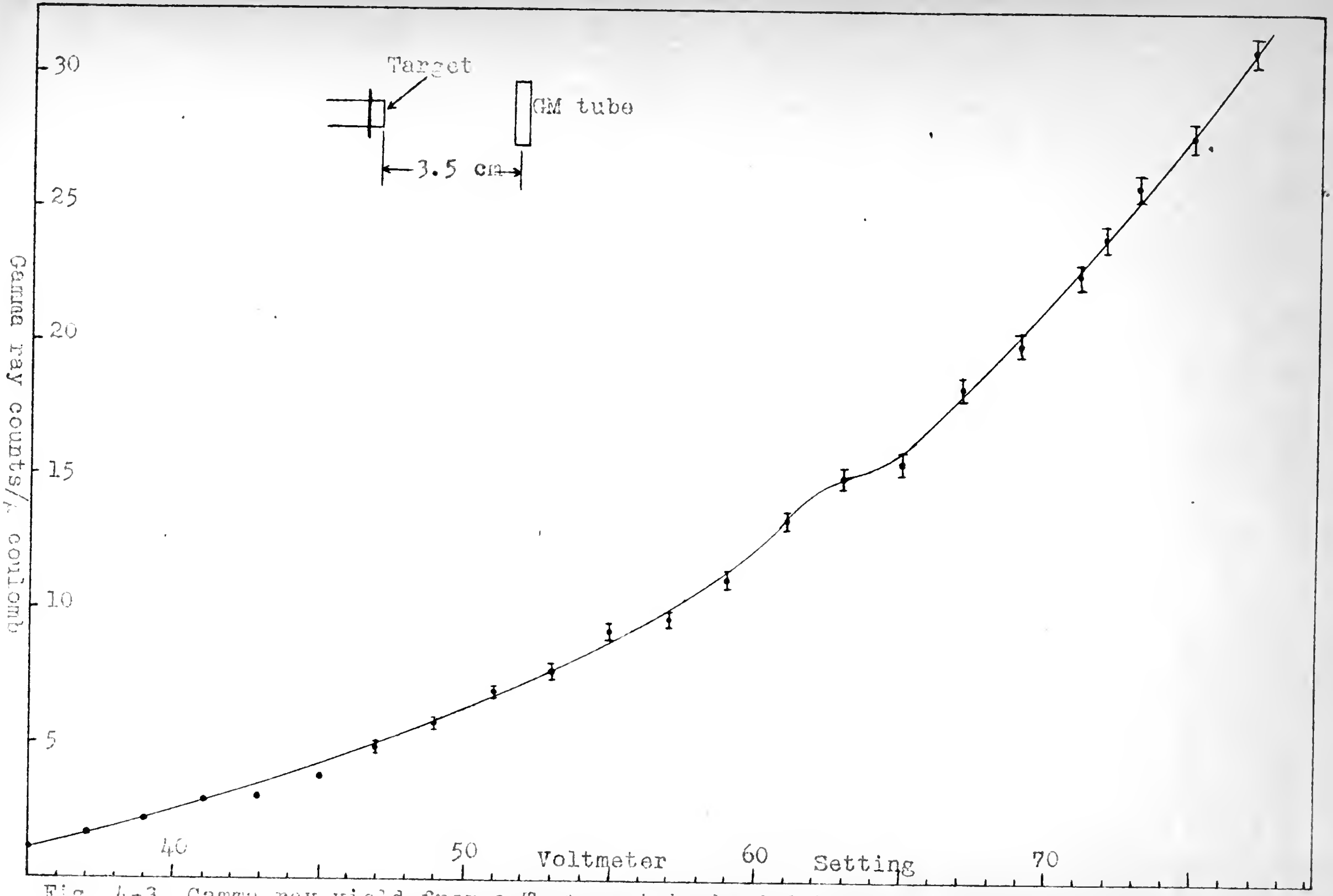

Fig. 4-3. Gamma ray yield from a Ta target bombarded by protons.

at times. This is particularly true for low intensity beams (0.5 μ amp or less). In some instances, it has been found possible to make data reproducible and consistent only by subtracting a background effect which is a linear time function. This correction was determined by repeating measurements at different beam intensities, so that varying amounts of time were required to collect a specified amount of charge on the target. Possible explanations of the effect lie in the presence of radioactive sources near the detecting equipment, or in leakage or non-linearity of the beam current integrator. The former cause is guarded against by removal of sources, while the latter has been tested by use of various known current sources as an input to the beam current integrator, with no defect being detected. The sources and distribution of background radiation will need careful investigation before precise cross section and energy measurements can be undertaken.

A long counter, similar to that described by Hansen and McKibben (Ha 47), was used as a neutron detector. The paraffin cylinder was 8" in diameter by 10" in length. However, no holes were provided in the face of the paraffin, as described in the reference. The counter itself has the following specifications:

Outside diameter	1"
Wall thickness	0.042" brass

Active volume	10" in length
Center wire	2 mil tungsten
Filling	55 cm-Hg of 96% enriched BF_3
Operating voltage	2200 volts

The gamma ray detector was a Victoreen 1B85 Thyrode Counter tube, with the following specifications:

Outside diameter	51/64"
Wall thickness	30 mg/cm^2 aluminum
Active volume	2.75" in length
Operating voltage	790 volts

CHAPTER V

PREPARATION OF TARGETS

During the course of these investigations, several different targets were used: a deuterium target, a lithium target, two vanadium targets, and a scandium target. Neither the deuterium target nor the lithium target presented any special problems. A deuterium target, consisting of deuterium gas absorbed in a layer of zirconium on a wolfram backing, described by Graves *et al.* (Gr 49), was available. The rotating target holder of the Rockefeller Generator is equipped with an electric furnace suitable for evaporating lithium targets *in situ.*

Vanadium, because of its high boiling point, 3000° C. (Fo 47), cannot be evaporated in the generator furnace. Baird Associates of Cambridge, Massachusetts were requested to prepare two targets of about 0.2 and 0.5 microns thickness. They experienced no difficulty in evaporating vanadium in vacuo. The method used was to insert a sliver of vanadium about 5 mm. x 3 mm. x 1 mm. into a closely wound helix of wolfram wire which was heated by conduction. This method has the disadvantage that the shadow of the wolfram helix makes the tar-

get somewhat non-uniform.

The problem of preparing a thin scandium target proved to be difficult. The only form of scandium which was available was the oxide, prepared by Johnson, Matthey and Company, Limited, of London, and certified, "spectrographically standardized". It was obtained from the Jarrell-Ash Company of Boston, Massachusetts. While the boiling point of metallic scandium, 2400° C. (Ho 47), is not excessive, the oxide is highly refractory, and temperatures high enough to reduce the oxide are difficult to attain. Because the material is a fine powder, the wolfram helix method is not suitable. O'Bryan (Ob 34) describes a technique for evaporating highly refractory substances. It consists essentially of bombarding a small carbon crucible with electrons accelerated by about 4,000 volts. This method was tried unsuccessfully. The limitation was the difficulty of attaining a vacuum sufficiently high to prevent the formation of a gas discharge.

A method was devised which was successful. A 1/4" graphite rod of spectroscopic purity was used. The rod was 4" long. The middle 2 inches were tapered down so that the cross section in the center was 1.5 mm. x 1.5 mm. A longitudinal groove about 1 mm. deep and 5 mm. long was cut in this small central cross section, forming a boat-like crucible. Heating currents of the order of 200 amperes are required. The ends of the graphite rod

operate at red heat and must be held by tantalum clamps to avoid melting the brass clamps which are ordinarily used. With this arrangement, the oxide was easily reduced and the metallic scandium deposited on the target by evaporation. The method is considerably simpler than O'Bryan's and avoids the necessity for high voltage and high vacuum.

CHAPTER VI

AN ENERGY LEVEL IN LI^7 FROM THE DISINTEGRATION OF BORON BY SLOW NEUTRONS

Introduction

The reaction $B^{10}(n,\alpha)Li^7$ produced by thermal neutrons leads either to the ground state or to an excited state in Li^7. The excited state decays to the ground state by the emission of a γ-ray. It is possible to observe α-γ coincidences from the disintegration of B^{10}. This experiment has been performed by Rose (Ro 48), who obtained a value of 0.48 ± 0.015 Mev for the γ-ray energy by absorption measurements in lead.

The objectives of the present investigation were: (1) to measure the energy of the Li^7 γ-ray as a check on published data, (2) to test the operation of the electronic circuit which had been developed, and (3) to demonstrate the usefulness of a fast coincidence circuit in the presence of a copious source of neutrons for determining levels formed by neutron bombardment and which decay by γ-ray emission.

Method

A sketch of the experimental arrangement appears in Fig. 6-1. The source of neutrons was a deuterium target bombarded by 1.4 Mev deuterons from the Rockefeller generator. The target was surrounded by a block of paraffin 20" x 12" x 6". A hole 2" in diameter and 3" deep was bored in the paraffin in order to introduce the target into the center of the block. The purpose of the paraffin was to moderate the fast neutrons from the target. The neutrons were slowed down because: (a) the neutron capture cross-section of B^{10} follows the familiar 1/v law, and therefore is a maximum for thermal neutrons, and (b) fast neutrons would be detected by the scintillation counter used to measure the γ-rays (these neutrons would increase the counting rate in the γ-ray channel and thereby increase the random coincidence rate, which dictates the sensitivity of this experiment).

In order to reduce still further the counting rate in the γ-ray channel, a wall of lead bricks 2" thick separated the paraffin block and the proportional counter. The purpose of this wall was to shield the scintillation counter from the γ-rays produced by neutron capture in the paraffin.

The proportional counter was of brass, outside diameter 1", active volume 3" long, center wire 2 mil tungsten, and 0.042" wall thickness, filled with boron triflu-

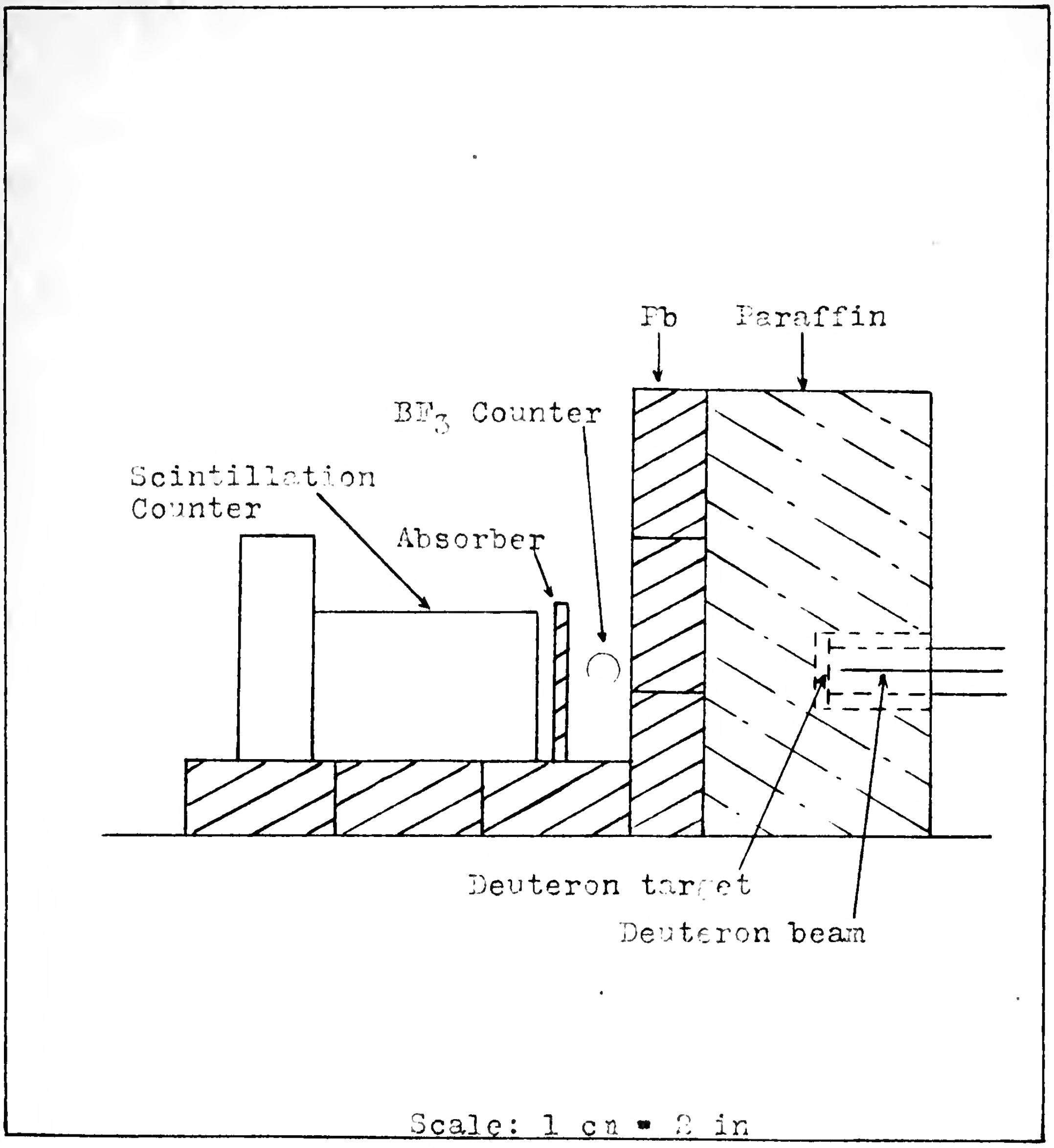

Fig. C-1. Experimental arrangement for Li^7 gamma ray coincidence absorption measurements.

oride (96% B^{10}) at a pressure of 21 cm. of mercury. The scintillation counter, amplifiers, coincidence circuit, and scalers were those described in Chapter II.

About 90% (Ro 48) of the Li^7 nuclei are formed in an excited state. The γ-rays accompanying the de-excitation of this state escape from the proportional counter and are detected by the adjacent scintillation counter. The energy of this γ-ray, corresponding to the energy of the excited state, was measured by comparing its absorption coefficient in lead (4" x 4" x 0.0645" sheets) with that of 0.51 Mev annihilation radiation from Cu^{64}. The absorption coefficient was determined by measuring the ratio of α-γ coincidences to the number of α pulses as a function of the thickness of lead absorber placed between the counters.

The total number of counts produced in each of the single channels and in the coincidence channel were observed. In addition, the total elapsed time for each run was recorded. Let

N_α = the total number of counts observed in the proportional counter channel.

N_γ = the total number of counts observed in the scintillation counter channel.

N_{CT} = the total number of coincidence counts observed.

N_T = the number of true coincidences.

N_C = the number of chance coincidences.

Δt = the elapsed time for a run.

τ = the resolving time of the coincidence circuit.

We wish to determine the ratio N_T/N_α as a function of the lead thickness. It is necessary to determine the number of chance coincidences which may be expected in order to find the number of true coincidences. In accordance with the usual formula for random coincidences (Du 40), the chance rate is

$$N_C/\Delta t = 2\tau(N_\alpha/\Delta t)(N_\gamma/\Delta t) \tag{6-1}$$

The chance coincidence rate increases with the product of the two single channel rates, which increase linearly with the beam current from the high-voltage generator. Therefore the chance rate varies as the square of the beam current, whereas the true coincidence rate varies as the first power. This second power dependence requires that the variation in beam current as a function of time during a run be known, if corrections for chance coincidences are to be made. To reduce this effect, the beam was held as constant as possible. It is not necessary to have the same beam current during each run, only that the beam current remain constant during a given run.

The customary procedure for determining τ is to observe the single channel rates and the coincidence rate using two independent sources. All coincidences observed must then be random coincidences. Substitution of the three rates into (6-1) gives τ. A slight variation of

this method was adopted. Instead of two sources, the boron fissions in the proportional counter were used as the source. To insure that all coincidence counts were due to chance, an additional length of delay line, equivalent to 0.15 μ seconds, was inserted in the proportional counter channel. This delay is considerably larger than the resolving time of the coincidence circuit (see Chapter II). Since the pulse in the proportional counter and the appearance of the Li^7 γ-ray are essentially simultaneous, the presence of this delay prevents any true coincidences being recorded. The results are given in the first row of Table 6-1. Substitution of the observed values into (6-1) gives:

$$2\tau = 0.66 \pm 0.07 \times 10^{-9} \text{ min.}$$

The extra delay was removed from the proportional counter channel, and a delay of 0.04 μ seconds inserted in the scintillation channel. This delay compensates for the average electron transit time in the proportional counter, which constitutes an intrinsic delay in this channel, as discussed in Chapter II. The total counts in both single channelsand the total coincidence counts were observed as a function of the thickness of lead interposed between the proportional counter and the scintillation counter.

Results

The errors shown in Table 6-1 are probable errors

due to statistical fluctuations in the total number of counts. The fractional probable errors in the single channel counts are negligible compared to those in the coincidence counts. The first row gives the results of the experiment from which 2 τ was determined. This value was used to compute the number of chance coincidences.

TABLE 6-1

No. of Lead Sheets	Δt (min)	N_α	N_γ	N_{CT}	N_C	N_T	N_T/N_α
Random Counts	29.90	526,848	3,948,800	46 ±4.6	46 ±4.6	0	0
0	34.37	503,232	4,268,800	643 ± 17	45 ±4.5	598 ±18	1.190×10^{-3} $\pm0.036\times10^{-3}$
1	20.50	452,288	3,654,400	441 ± 14	53 ±5.3	388 ±15	0.859×10^{-3} $\pm0.033\times10^{-3}$
2	25.82	539,584	4,249,600	416 ± 14	56 ±5.6	360 ±15	0.688×10^{-3} $\pm0.028\times10^{-3}$
3	26.15	530,624	4,096,000	302 ± 12	55 ±5.5	247 ±13	0.465×10^{-3} $\pm0.024\times10^{-3}$
4	24.38	522,624	3,872,000	255 ± 11	55 ±5.5	200 ±12	0.383×10^{-3} $\pm0.023\times10^{-3}$
5	29.98	586,240	4,256,000	212 ± 10	55 ±5.5	157 ±11	0.268×10^{-3} $\pm0.019\times10^{-3}$
6	36.62	740,288	5,248,000	240 ± 10	70 ±7.0	170 ±12	0.230×10^{-3} $\pm0.016\times10^{-3}$
7	46.02	904,064	6,227,200	227 ± 10	81 ±8.1	146 ±13	0.162×10^{-3} $\pm0.014\times10^{-3}$
8	34.60	649,280	4,569,600	128 ± 8	57 ±5.7	71 ±10	0.110×10^{-3} $\pm0.015\times10^{-3}$
9	38.60	703,616	4,736,000	102 ± 7	57 ±5.7	45 ± 9	0.064×10^{-3} $\pm0.013\times10^{-3}$

These results are plotted in Fig. 6-2. The best fit gives $\mu = 1.7 \pm 0.1$ cm^{-1}, the probable error being estimated by inspection.

Using the above value of μ and the γ-ray absorption coefficients provided in M.I.T. Course 8.512*, it is possible to estimate the energy as about 0.5 Mev. The geometry of the experiment is "poor", hence this is not an accurate value of the γ-ray energy since the contribution of the Klein-Nishina scattering to the total observed absorption coefficient is uncertain. This contribution may vary from zero, for ideal spherical geometry, to a maximum (the value plotted in the curves) for ideal narrow beam geometry.

In order to determine the fraction of the Klein-Nishina scattering which is effective, the absorption coefficient of a γ-ray of known energy is measured in the same geometry as was the unknown. The reference γ-ray should have an energy approximately equal to that of the unknown. The γ-rays from Cu^{64} are almost pure annihilation radiation (0.51 Mev); harder γ's are present to the extent of only one 1.35 Mev quantum per 40 ± 5 positrons (De 47).

A source of Cu^{64} was prepared by bombarding copper with deuterons in the cyclotron for five minutes, and allowing it to stand for four hours to remove the five minute activity of Cu^{66}. The copper was dissolved in nitric acid

---

*These curves constitute the latest revision of those appearing in R.D. Evans and R.O. Evans, "Studies of self-absorption in gamma-ray sources", Rev. Mod. Phys. <u>20</u>, 305-326 (1948).

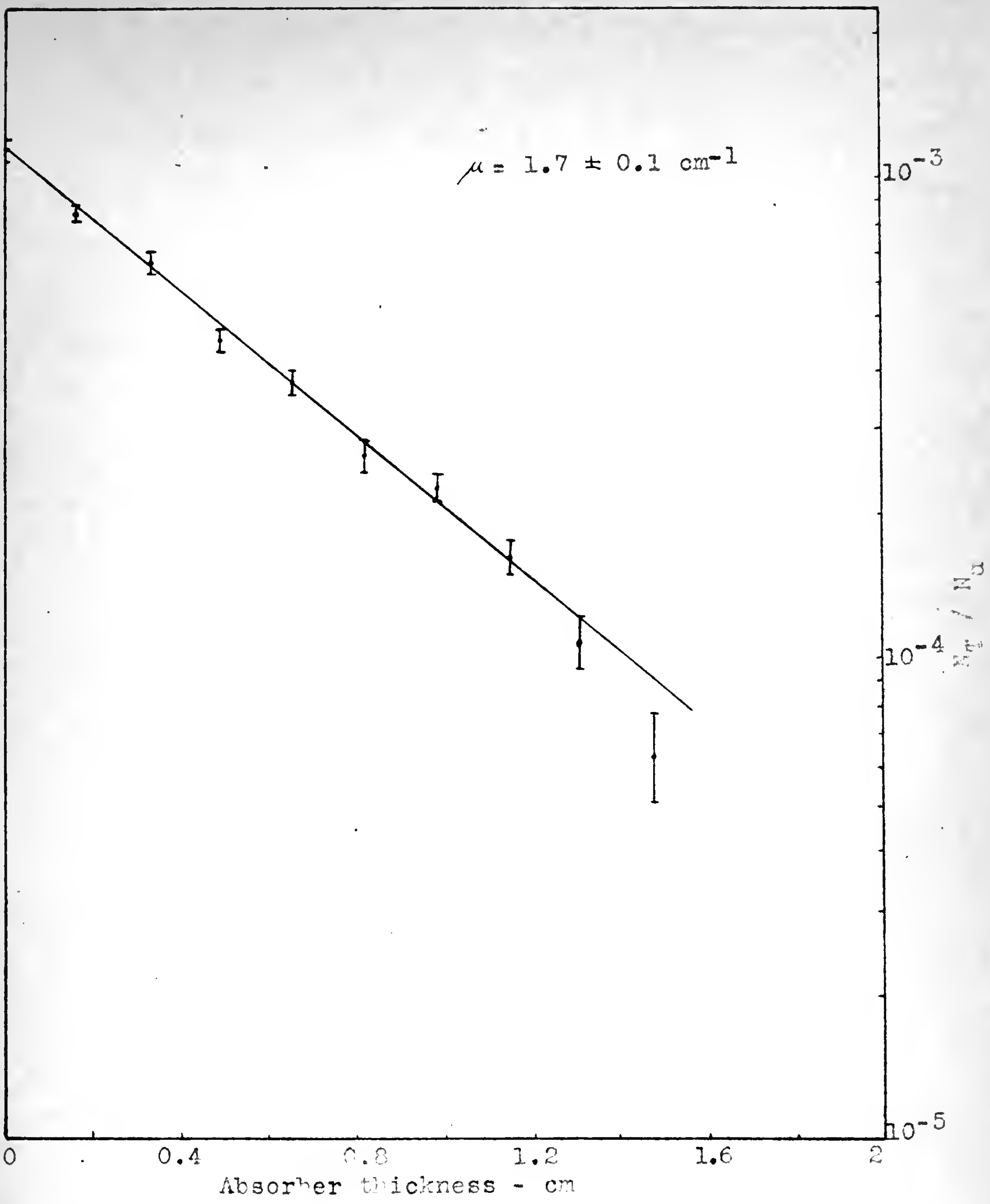

Fig. 6-2. Ratio of α-γ coincidences to neutrons detected (N_T/N) as a function of lead absorber thickness.

and electroplated on a platinum electrode to remove any zinc and nickel. From the electrolytic copper a concentrated solution of copper sulphate was prepared. These operations were performed by Mr. M.T. Corriveau of the Minerals Dressing Laboratory.

A dummy counter was made from the same tubing as the proportional counter. Its length was equal to the active length of the proportional counter. It was capped at each end with brass discs 0.05" thick, and coated on the inside with glyptal to prevent copper ions from being deposited on the walls. The dummy was filled with the copper sulphate solution, diluted to fill the volume, and was substituted for the proportional counter. The absorption coefficient for the annihilation radiation was measured, using the same equipment as before. The results, corrected both for background and for decay of the Cu^{64} source, are tabulated below. The probable errors due to statistical fluctuations were less than 1.0% for all thicknesses of lead.

TABLE 6-2

Number of Absorbers	Counting Rate per Minute
0	24,337
1	19,100
2	15,200
3	11,800
4	9,125
5	7,100
6	5,310
7	4,110
8	3,265
9	2,540

The best fit in Fig. 6-3 gives $\mu = 1.525 \pm 0.015$ cm^{-1}. The probable error was again estimated by inspection, and is negligible in comparison with the error in μ for the Li^7 γ-ray.

From the curves for lead, the maximum total absorption coefficient $\mu_c = 1.675$ cm^{-1} for 0.51 Mev γ-rays. The difference of 0.150 between this value and 1.525 cm^{-1}, as found above, is attributed to the poor geometry. The maximum value of the Klein-Nishina scattering coefficient σ_s for this energy is 0.51 cm^{-1}. Subtracting 0.15, we find 0.36 cm^{-1}, i.e., only 71% is effective. In the region of energies under consideration, the Klein-Nishina absorption coefficient, σ_a, has a constant value of 0.27 cm^{-1} and σ_s

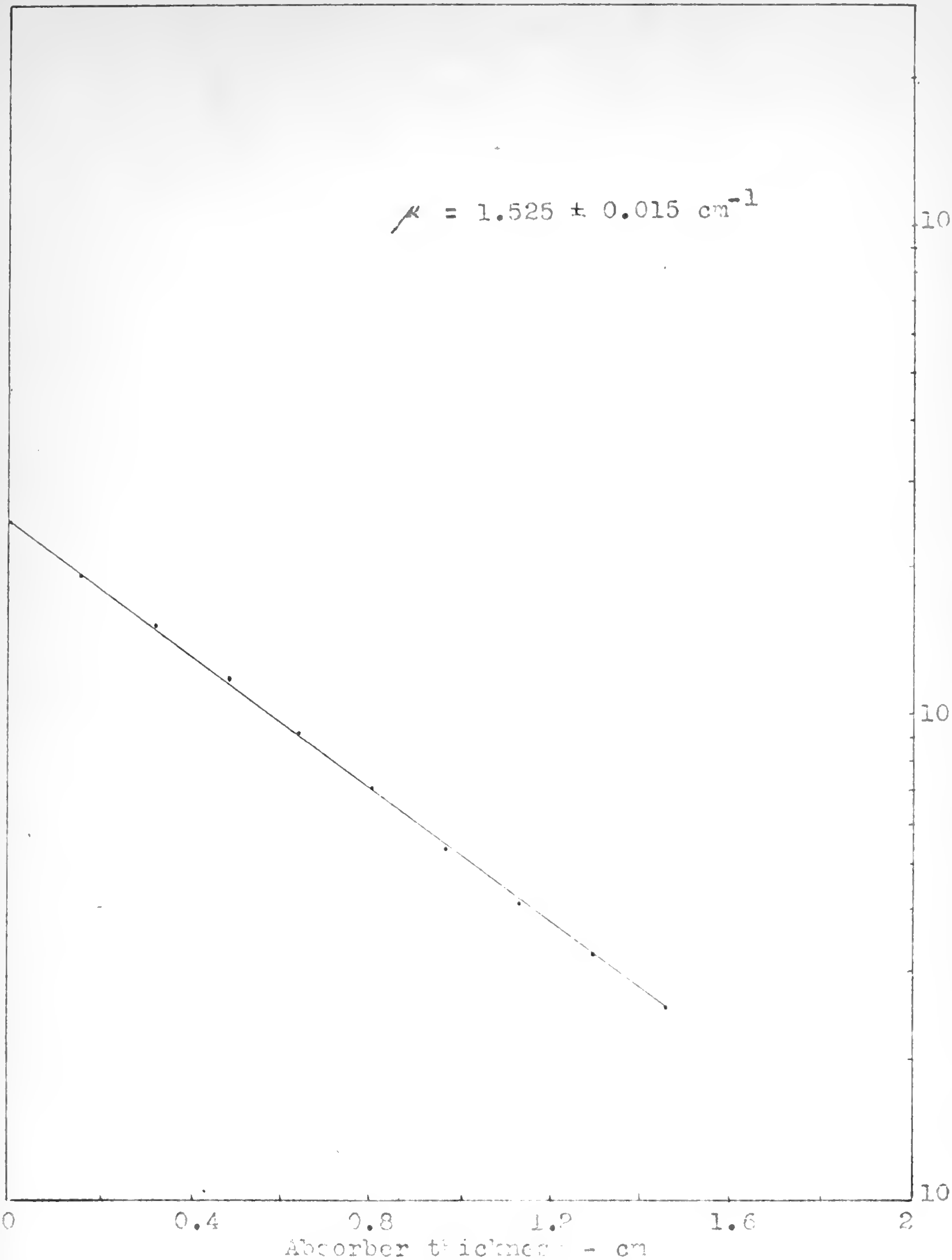

Fig. C-3. Dummy counter calibration - Cu^{64} annihilation radiation absorption in lead.

varies only slowly with energy. Hence, as a first approximation for the Li^7 γ-ray energy, σ_s may be taken as 0.36 cm^{-1}. The total Klein-Nishina coefficient $\sigma = \sigma_a + \sigma_s = 0.63$ cm^{-1}. Subtracting this from 1.7 cm^{-1} gives a photoelectric absorption coefficient of 1.07 cm^{-1} for Li^7 γ's, which corresponds to 0.48 Mev. A second approximation may be made by taking the effective σ_s as .79 x 0.53 cm^{-1} = 0.38 cm^{-1}, and proceeding as before. However, this slight correction makes no appreciable difference in the energy determination.

To estimate the probable error, the same procedure is applied using 1.8 cm^{-1} and 1.6 cm^{-1}, the observed upper and lower limits for the absorption coefficient of the Li^7 γ-ray. The energies found are 0.46 and 0.50 Mev. Accordingly, the energy of the Li^7 γ-ray is estimated as 0.48 ± 0.02 Mev in excellent agreement with Rose's value of 0.48 ± 0.015 Mev.

Discussion

A summary of work carried out before 1940 on the excited state of Li^7 appears in Graves' article (Gr 40). Work to 1947 is discussed by Siegbahn (Si 46, Si 47). More recent work is tabulated by Rose (Ro 48). The more recent values appear to be the most accurate, and center around 0.48 ± 0.01 Mev.

The probable error ascribed to the present determination is larger than that of many of the other determina-

tions. The source of this error, $\sim 5\%$, is mainly in the statistical fluctuations of the coincidence counting rates. Counting periods of about one-half hour were used, and only one run was made with each thickness of absorber. This is to be compared with the experiment performed by Rose (Ro 48) in which as many as five runs were made, some being sixteen hours long, in order to achieve 2% accuracy. The present method is inherently capable of greater accuracy. By devoting more time to experiments of this type, accuracies of better than 5% could be achieved. In view of the excellence of the previous work on Li^7, extended experiments did not seem justified in the present case.

CHAPTER VII

ENERGY LEVELS IN Be^8 AND Li^7 AS DETERMINED FROM THE BOMBARDMENT OF Li^7 WITH PROTONS

Introduction

Nuclear reactions resulting from the bombardment of Li^7 with protons have been studied extensively for several reasons:

a. The threshold for neutron production is low (1.881 Mev);

b. The reaction is a copious source of monoenergetic neutrons;

c. The pure metal is easily obtained, and targets of any desired thickness may be readily evaporated.

Mattauch and Flammersfeld (Ma 49) give a complete bibliography of these studies as of the end of 1948. Perhaps the most definitive work is that of Hornyak and Lauritsen (Hl 48) which consists of a compilation and coordination of results of many authors. Since the reactions using Li^7 are so well known, the study of them is particularly important for calibrating and evaluating the performance of the Rockefeller Generator.

The Gamma Ray Yield

The gamma ray yield curve, Fig. 7-1, was obtained using a target about 15 kev thick. Many resonances for formation of the compound nucleus Be^8 are exhibited, some of which have been previously reported. The possibility exists that some of these resonances result from impurities in the lithium. Metal Hydrides, Inc. of Beverly, which supplies the metal, lists these impurities as: Na, .6%; Ca, .02%; K, .01%; N, .06%; and Fe, .001%.

Using Fig. 7-1 and the reactions

$$Be^9 + p \rightarrow Be^8 + d + 0.558 \text{ Mev} \qquad \text{(Tl 49)}$$

$$\text{and} \quad Be^9 + d \rightarrow Li^7 + \alpha + 7.145 \text{ Mev} \qquad \text{(Bu 49)}$$

which have reliably determined Q values, the tentative energy level diagram, Fig. 7-2, has been constructed.

The level at 18.12 Mev results from inelastic scattering of the incident proton. As indicated in Fig. 7-2, the outgoing proton may leave the resultant Li^7 nucleus in an excited state at 0.48 Mev, which subsequently decays by gamma emission. The energy of this gamma ray was determined by simple absorption in lead, as described later. An independent means of arriving at this gamma ray energy has already been described in Chapter VI. The level at 18.36 Mev must be regarded with some doubt, since many accelerators have been able to reach a bom-

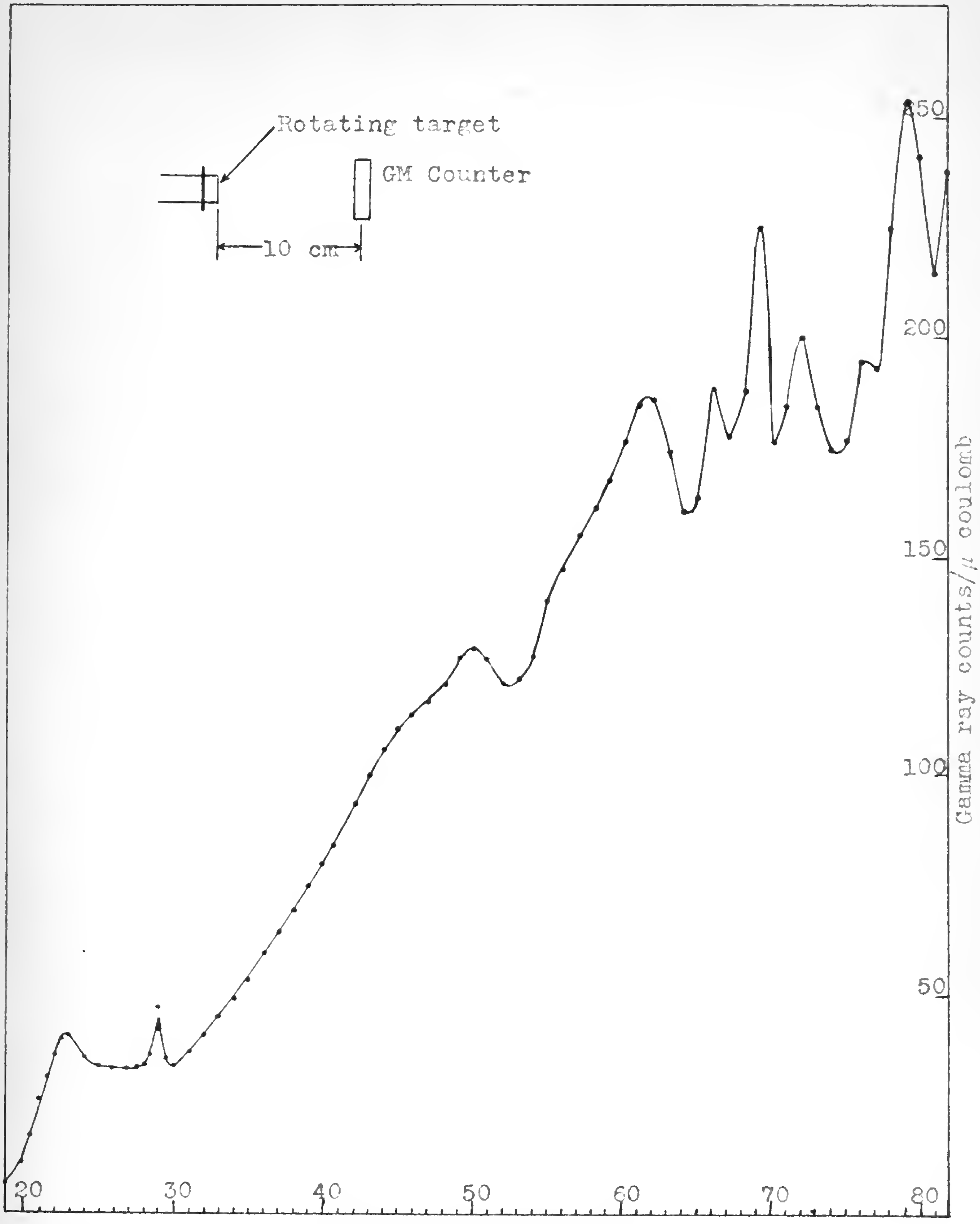

Fig. 7-1 . The gamma ray yield from a Li target bombarded by protons.

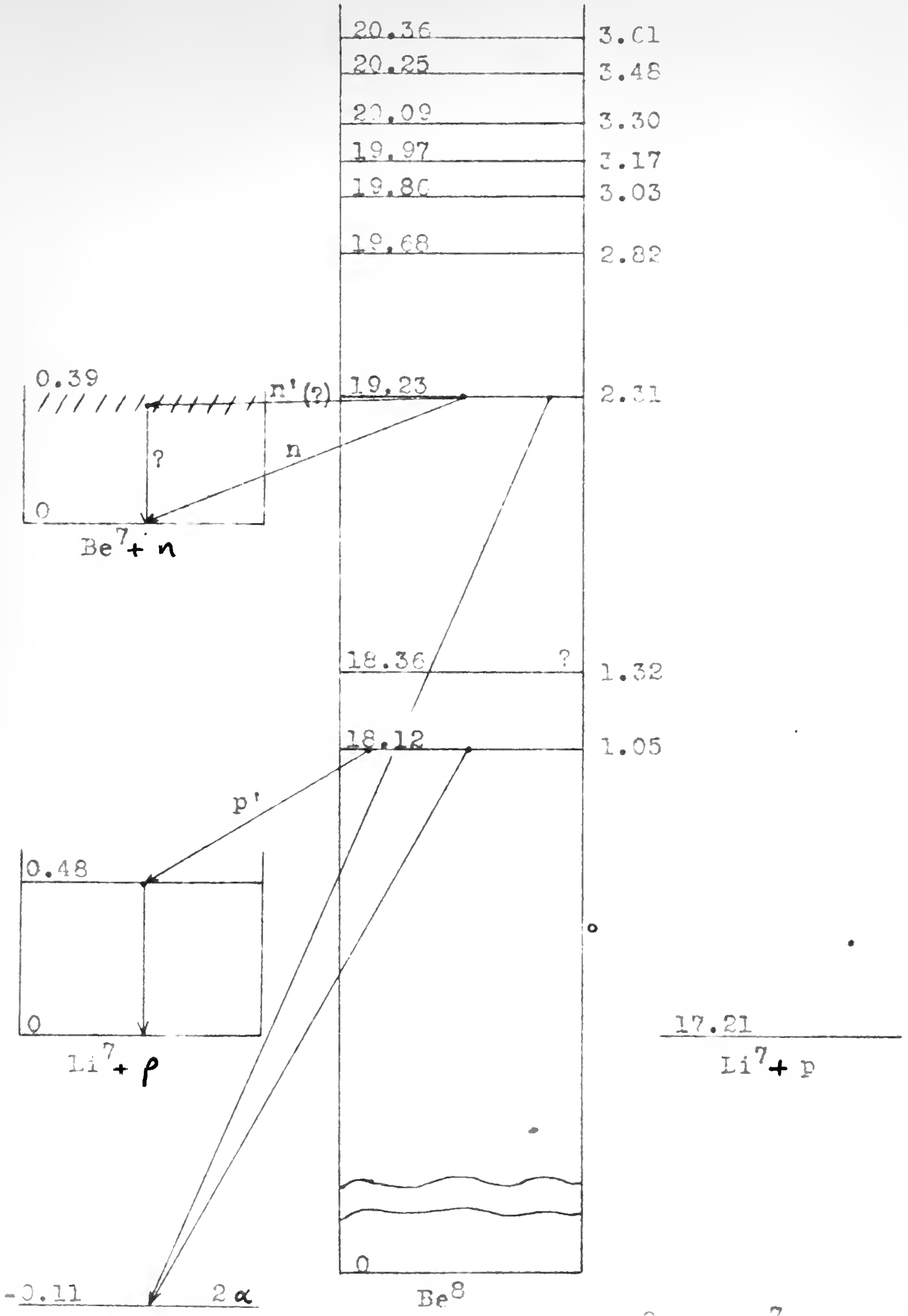

Fig. 7-2. Energy levels in the nuclei Be^8 and Li^7, showing only those determined in the present investigation. Numbers to the right of a level indicate proton bombarding energy.

barding energy of $E_p = 1.32$ Mev and this region of excitation has presumably been well investigated. The level was duplicated several times, using the same target, and using a different target. Since the fractional standard deviation of the data recorded was about 1 per cent, it is concluded that the level definitely does exist, although it can not be stated positively that it does not belong to some target impurity.

The level at 19.23 coincides with a resonance for neutron production. That there should also be a gamma resonance indicates

a. This level has two competitive modes of decay: one by gamma emission to the ground state; the other by emission of a neutron, leaving Be^7 in the ground state as a product nucleus;

or b. Since this level is believed <u>not</u> to decay to some lower level of Be^8 (Hl 48), another explanation of the gamma peak is that a neutron may be emitted, leaving the product nucleus Be^7 in an excited state, which subsequently decays by gamma emission.

This latter possibility, indicated by question marks on the level diagram, would give one a level in Be^7. From the diagram, it can be seen that if the neutron were emitted with essentially zero energy, the level in Be^7 would be $\sim$ 0.39 Mev above the ground state. By analogy with Li^7, which is the mirror nucleus of Be^7, one would expect a level of nearly this value to exist in Be^7. Recently, experimental evidence has been accumu-

lated indicating that such a level does exist (La 50, Jo 50) at 430 kev above the ground state. Grosskreutz and Mather (Gr 50) have found levels in Be^7 at 205, 470, and 745 kev above the ground state. However, some doubt has been cast upon their results.

The modes of decay of the levels at 19.68 Mev and above are only speculative. Not enough energy is available for the compound nucleus to split into $H^3 + He^4 + H^1$. The neutron yield in this region of bombarding energy indicates that the compound Be^8 nucleus has essentially a constant probability for decaying to Be^7 by neutron emission. It seems unlikely, however, that these levels decay by gamma emission to some lower state of Be^8, with subsequent splitting of the nucleus into two alpha particles.

Application of Wilson's Spherical Shell Model

The success of Wilson's spherical shell model of nuclei (discussed more fully in Chapters VIII and IX) in calculating the resonances in Cr^{52} and Ti^{46} led to attempts to fit it to Be^8 as well. As with other theories in which nuclei are regarded as liquid drops, Wilson's may be expected to show deviations for the light nuclei. Reasonable agreement can be achieved between observed and calculated resonances if one of the constants of Wilson's original equation (cf. Chapter VIII) is altered as

follows:

$$E_{nj} = 0.386\left[(n-1)(n+2)\right]^{1/2} + (1.44)(AZ^4)^{-1/3}(j)(j+1)$$

The change of the constant from .387 to .386 is equivalent to saying that the value of the $(Li^7 + H^1) - Be^8$ mass difference used in determining the observed levels is too low by 0.000055 amu. Table 7-1 shows the comparison between observed and calculated resonances.

TABLE 7-1

E_{obs}(Mev)	E_{nj}(Mev)	n	j
18.12	18.156	46	1
18.36	18.316	47	0
19.23	19.173	49	1/2
19.68	19.700	50	1
19.86	19.860	51	0
19.97	19.945	51	1/2
20.09	20.086	51	1
20.25	20.246	52	0
20.36	20.331	52	1/2

Since the error in determining the observed resonances is about 25 kev, the above table shows that the agreement between observed and calculated values for the levels is about as well as can be expected for such a light nucleus as Be^8.

Li^7 γ-Ray Absorption Measurements

The energy of the γ-ray corresponding to the resonance observed at 1.05 Mev proton energy was measured by absorption in lead. With the generator operating at 1.05 Mev, lead sheets 4" x 4" x 0.0645" were interposed between the target and Geiger-Mueller counter. The absorption curve, corrected for background, is shown in Fig. 7-3. The probable errors indicated are 0.6745 times the standard deviation of a single observation. The best fit gives $\mu = 1.55 \pm 0.05$ cm^{-1}, the error being estimated by inspection.

Here again, as in the measurements described in Chapter VI, the geometry is "poor", and calibration is necessary. A source of Cu^{64} annihilation radiation was prepared by bombarding a sheet of copper for two minutes in the cyclotron. A strip 1 mm. x 2 mm. was cut out and placed on a tantalum target at the point ordinarily struck by the beam. The previous geometry was duplicated in all respects. The results of the calibration measurement, corrected for background and for source decay, are plotted in Fig. 7-4. The probable errors are about 1% for all points. From the figure, $\mu = 1.46 \pm 0.02$ cm^{-1}, the error being estimated by inspection.

Computations identical with those described in detail in Chapter VI yield 0.49 ± 0.01 Mev for the

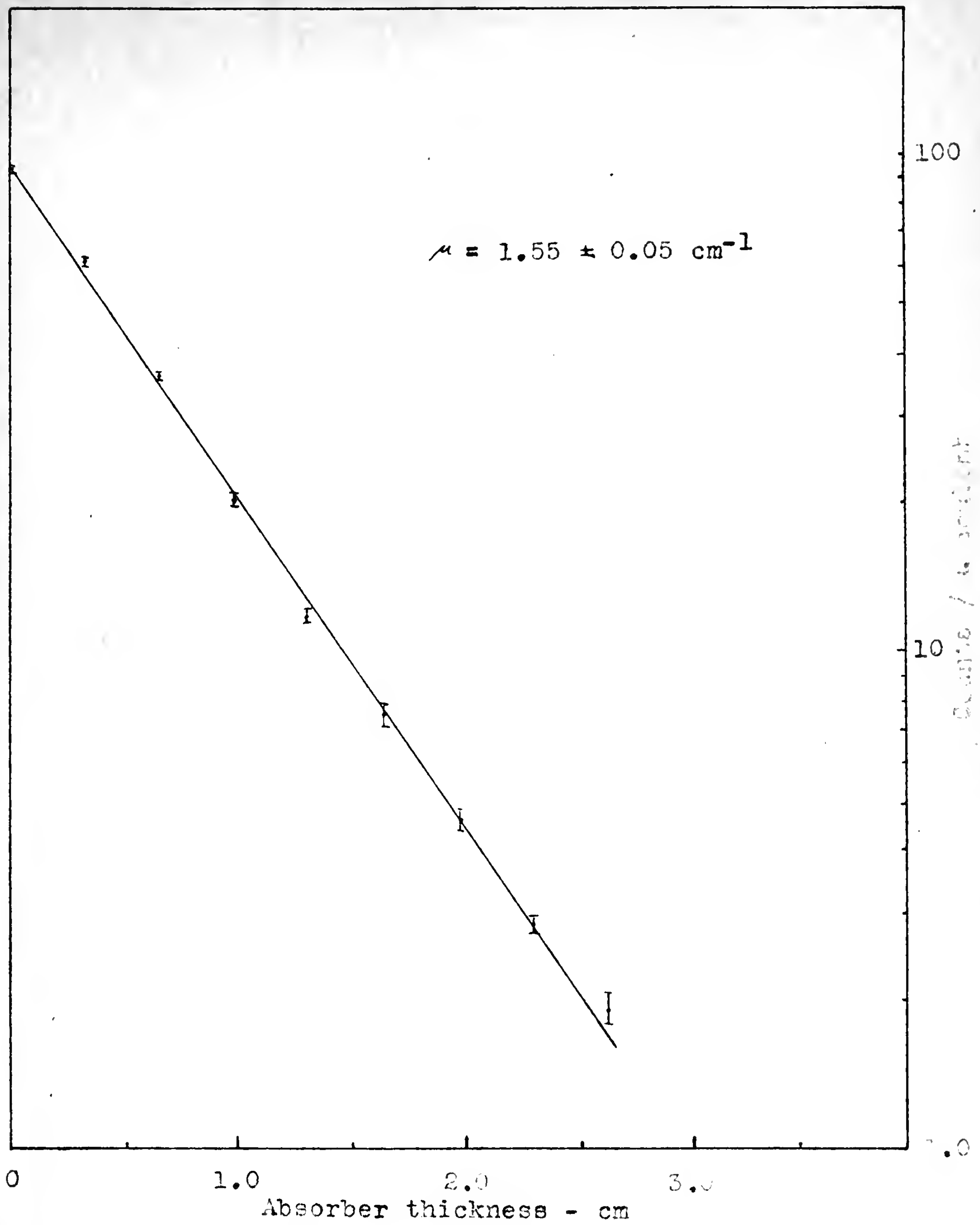

Fig. 7-3. Li^7 γ-ray absorption in lead.

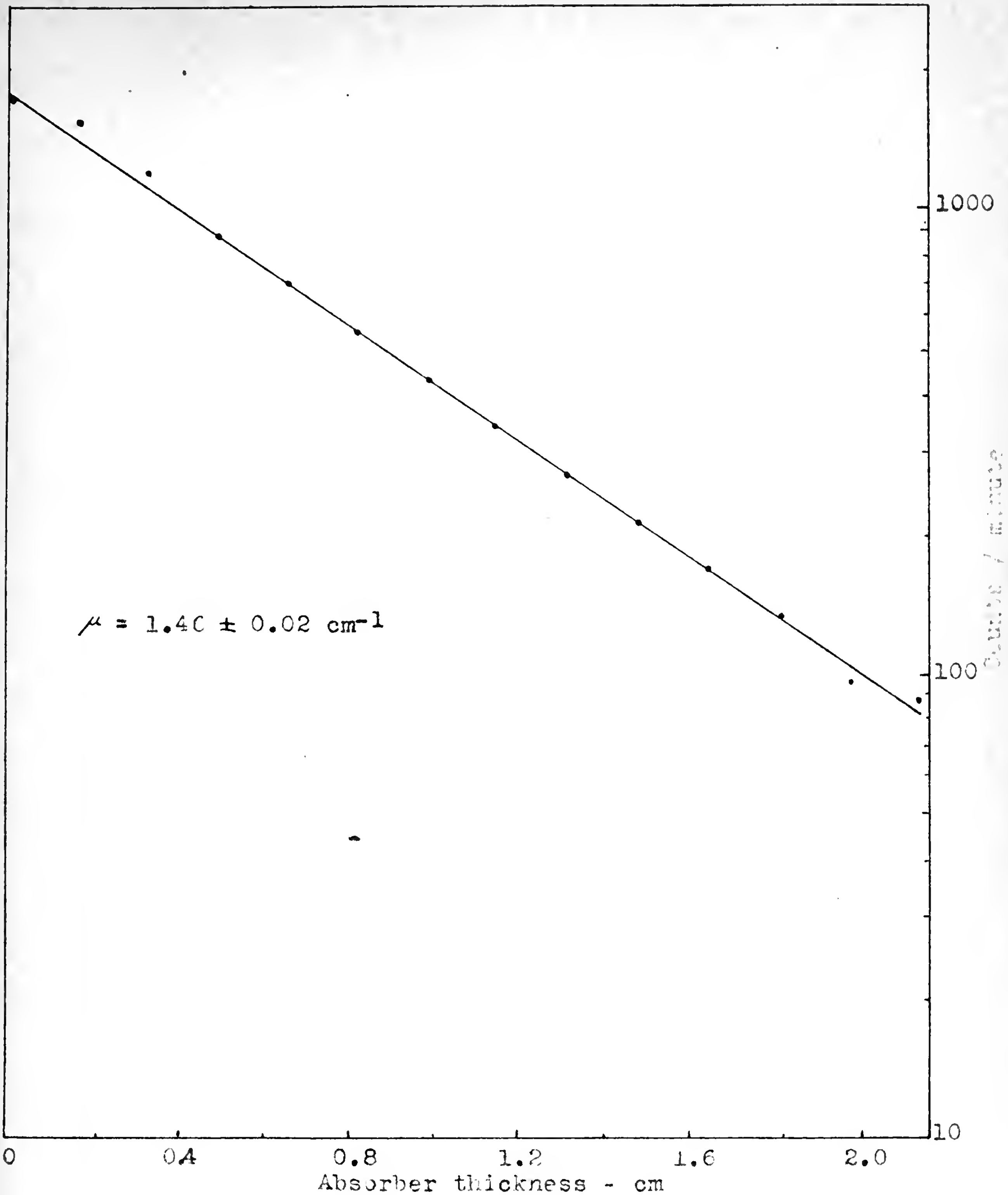

Fig. 7-4. Calibration measurement - Cu^{64} annihilation radiation absorption in lead.

energy of the Li^7 γ-ray, agreeing, within the experimental errors, with the value found in Chapter VI and the values of other workers cited in that chapter.

CHAPTER VIII

ENERGY LEVELS IN Cr^{52} AS DETERMINED FROM THE BOMBARDMENT OF V^{51} WITH PROTONS

Introduction

To date, the reaction $V^{51}(p,n)Cr^{51}$ has received only scant attention. Bradt (Br 45) and co-workers used the reaction to study the radiation from Cr^{51}. In 1948, Smith and Richards (Sm 48), using a target of V_2O_5, found the threshold for neutron production at $E_p = 1.564 \pm 0.003$ Mev. Recently, Hanson and Taschek (Ha 48) measured the neutron yield from a thick vanadium target for energies up to $E_p = 2.9$ Mev, and from a thin target for energies up to 2.0 Mev. We have confirmed Hanson and Taschek's results for thick targets, and have extended the measurements for both thick and thin targets to $E_p = 3.7$ Mev.

The study of reactions involving medium weight nuclei such as V and Sc is important for several reasons:

a. The neutrons from the target have low energy near the threshold.

b. There is only a small variation in energy of the neutron beam with angle.

c. The low energy neutrons are emitted in

the forward direction, in contrast with the neutrons from $Li^7 + p$ in which neutrons of comparable energy are emitted at backward angles. The background of back scattered neutrons which occurs with the latter reaction is thus effectively eliminated.

d. With sufficient energy resolution of the proton beam and very thin targets, i.e., only a few kilovolts, one can obtain considerable information concerning the level widths and level spacing, thus providing a check on theory.

Thick Target Yield

A thick vanadium target was prepared using a sliver of the metal approximately one millimeter thick. The metal contained 10% iron, with only traces of other impurities.

The yield curve in Fig. 8-1 indicates a threshold of 1.56 ± 0.01 Mev. The probable error is the result of the uncertainty in beam energy as discussed in Chapter IV.

A plot of the Gamow penetration factor

$$G = \frac{\alpha}{e^{\alpha} - 1}$$

where

$$\alpha = \frac{4 z Z e^2}{\hbar v} \left\{ \arccos \sqrt{x} - \sqrt{x(1 - x)} \right\}$$

and

$$x = \frac{ER}{z Z e^2} = \frac{E}{B}$$

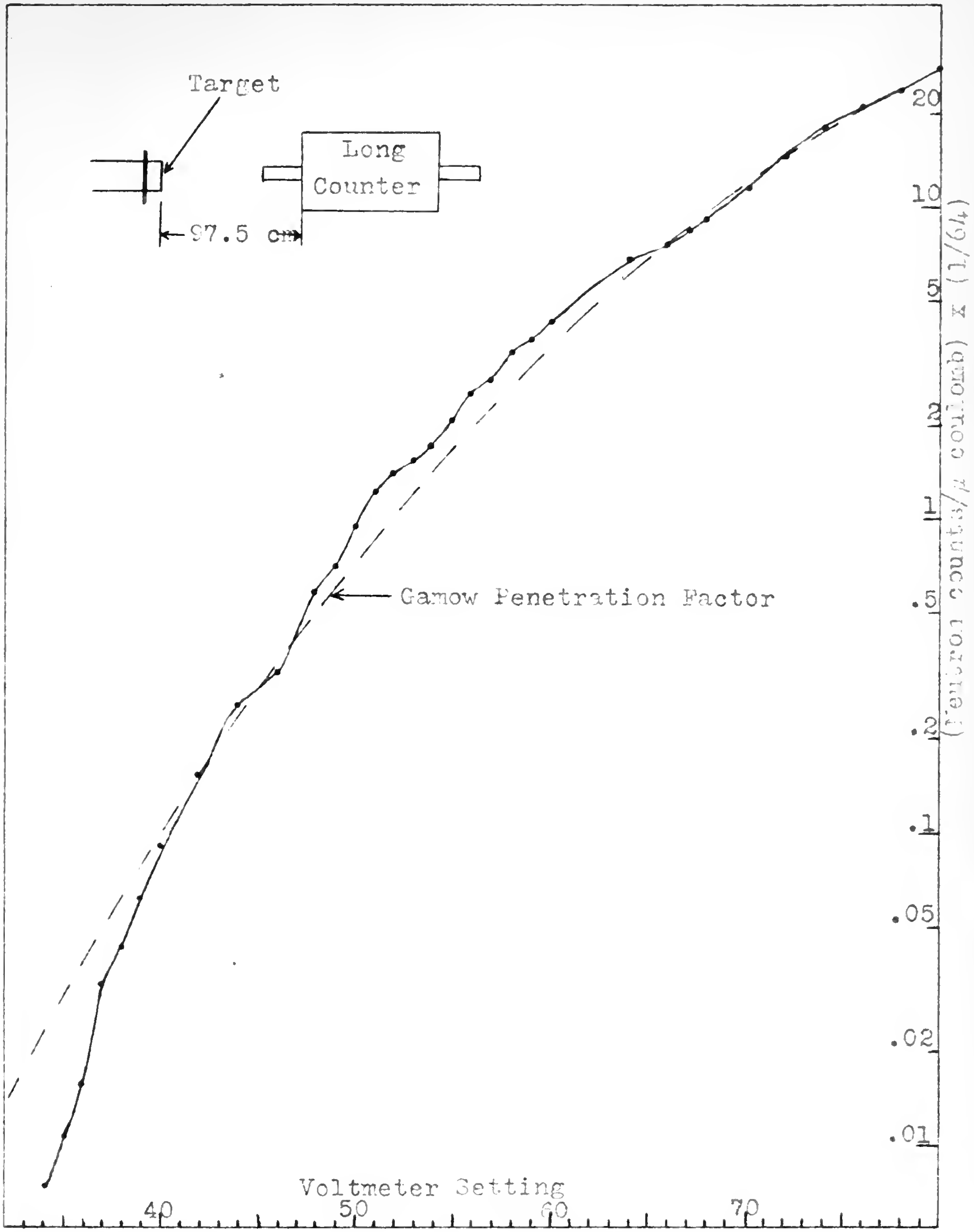

Fig. 8-1. Neutron yield from a thick vanadium target bombarded by protons.

has been superposed on the neutron yield curve of Fig. 8-1. The two plots are normalized at a generating voltmeter setting of 80. Since the energy of the bombarding proton never reaches the top of the coulomb barrier of the vanadium nucleus (about 6.25 Mev), the yield is seen to increase very nearly as predicted.

Thin Target Yields

Two thin vanadium targets were prepared by Baird Associates by evaporation in vacuo. The first, 5000 Å (42 kev) in thickness, gave a neutron yield with indications of several resonances. To investigate these resonances more thoroughly, the thinner target (17 kev) was used although its surface was somewhat crazed. The results are given on a semi-log scale in Fig. 8-2. Fig. 8-3, a linear plot of the same data, emphasizes the resonances obtained. No attempt has been made to indicate the statistical error, since for most points the fractional standard deviation is only about 1 per cent. Near threshold, it rises rapidly to about 5 per cent. An attempt was made to establish each resonance by three points on either side of the peak. However, the resolution of the generator was not sufficient in some instances. Table 8-1 is derived from Fig. 8-3.

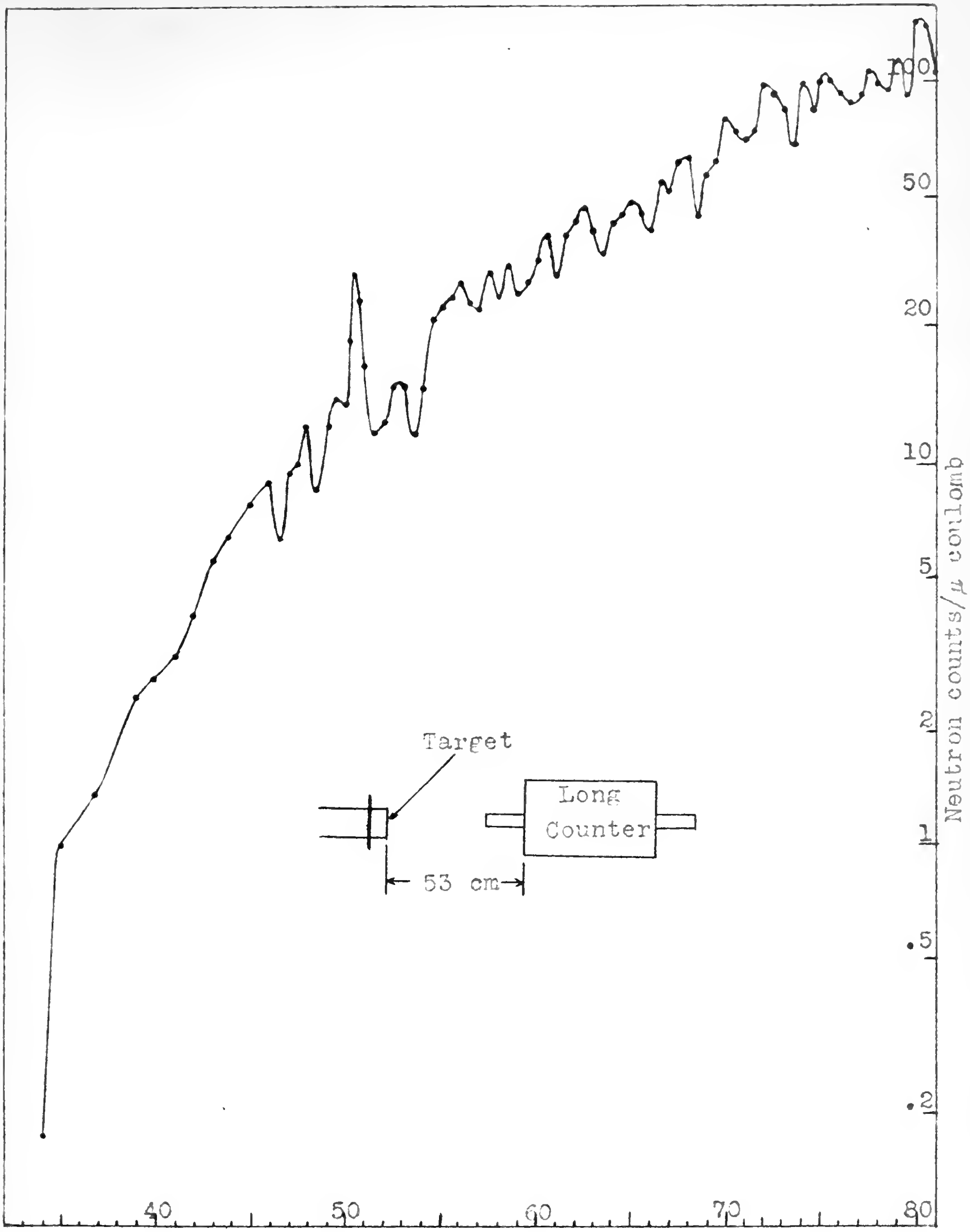

Fig. 8-2. Neutron yield from a thin (17 kev) vanadium target bombarded by protons.

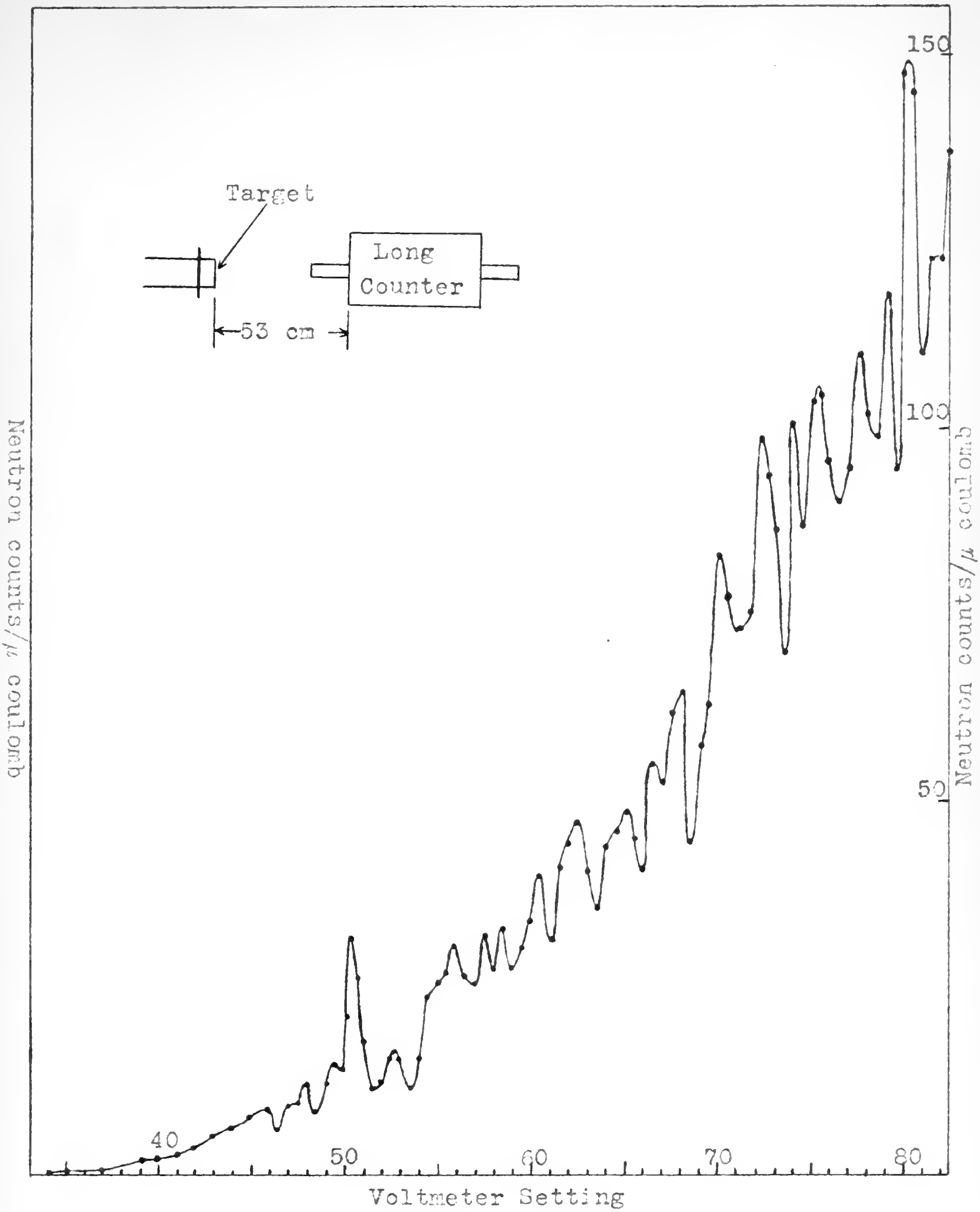

Fig. 8-3. Neutron yield from a thin (17 kev) vanadium target bombarded by protons.

TABLE 8-1

Generating Voltmeter (arbitrary)	Proton Energy (Mev)	$\frac{M_2E_1}{M_1 + M_2}$ (Mev)	E_{52} (Mev)
46	2.13	2.09	11.34
48	2.22	2.18	11.43
49.5	2.28	2.24	11.49
50.5	2.33	2.28	11.53
52.75	2.43	2.38	11.63
56	2.58	2.53	11.78
57.5	2.645	2.59	11.84
58.5	2.69	2.64	11.89
60.5	2.78	2.72	11.97
62.5	2.87	2.82	12.07
65	2.985	2.93	12.18
66.5	3.05	2.99	12.24
67.75	3.105	3.04	12.29
70	3.21	3.15	12.40
72	3.30	3.24	12.49
74	3.39	3.33	12.58
75.25	3.45	3.38	12.63
77.5	3.55	3.48	12.73
79	3.62	3.55	12.80
80.25	3.68	3.61	12.86
81.75?	3.74?	3.67?	12.92?

E_{52} represents the energy levels in Cr^{52}, obtained from:

$$E_{52} = (M_2 + M_1 - M_c)c^2 + \frac{M_2E_1}{M_1 + M_2} .$$

M_1 and M_2 = masses of bombarding and target nuclei respectively, E_1 = energy of the bombarding particle, M_c = mass of the compound nucleus in its ground state. To compute E_{52}, the masses of Cr^{52} and V^{51} as given by Segre (1948) have been used. The uncertainty in these mass differences is of the order of 1 Mev. Hence, the absolute values of E_{52} also may be in error by this a-

mount. However, the calculated separations of the levels should be accurate to within about 15 kev.

Fig. 8-3 indicates that many of the resonances have widths at half maximum of about one half scale division on the generating voltmeter ~ 27 kev. Since the target was ~ 17 kev in thickness, we have approximately 10 kev as an upper limit for the actual level width. The average level spacing is ~ 80 kev.

The data of Table 8-1 have been used to construct a rough energy level diagram, Fig. 8-4. Transitions from certain excited levels of Cr^{52} to the ground state of Cr^{51} have been indicated as probable while other levels are believed to decay to an excited state of Cr^{51} based on the gamma ray yield curve described later.

According to the spherical shell model of nuclei of Wilson (Wi 50), the excited levels of a nucleus are given by

$$E_{nj} = 0.387\left[(n - 1)(n + 2)\right]^{1/2} + 1.44(AZ^4)^{-1/3}(j)(j + 1)$$

The general form of the equation has been computed according to the classical method of Rayleigh (Ra 79) for finding the modes of vibration and rotation of a water droplet. The constants have been found empirically by Wilson to satisfy known levels in certain nuclei. Using Wilson's equation, various values of n and j have been assumed to see if the theory agrees with the observed levels in vanadium.

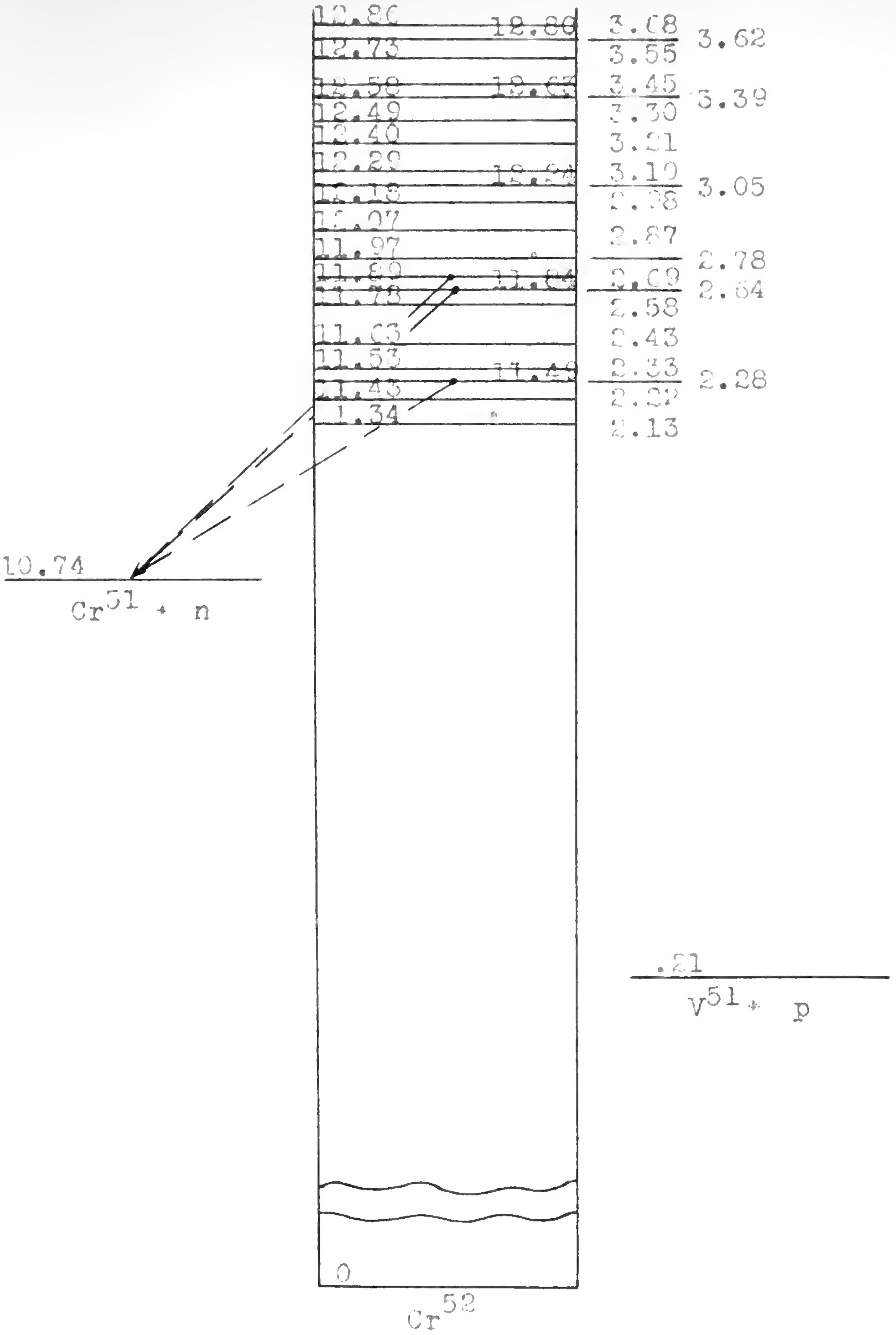

Fig. 8-4. Energy levels of Cr^{52}, showing those determined in the present investigation. Numbers to the right of a level indicate bombarding energy.

The results are given in Table 8-2.

TABLE 8-2

Observed level (Mev)	E_{nj} (Mev)	n	j
11.34	11.327	28	7
11.43	11.402	29	0
11.49	11.469	29	3
11.53	11.513	29	4
11.63	11.636	29	6
11.78	11.789	30	0
11.84	11.856	30	3
11.89	11.900	30	4
11.97	11.956	30	5
12.07	12.023	30	6
12.18	12.177	31	0
12.24	12.244	31	3
12.29	12.289	31	4
12.40	12.411	31	6
12.49	12.489	31	7
12.58	12.564	32	0
12.63	12.631	32	3
12.73	12.731	32	5
12.80	12.798	32	6
12.86	12.876	32	7

The agreement is remarkably good, especially since the probable error in an observed level is ± 15 kev. However, as Wilson points out, values for n and j may be selected so that the calculated levels fit nearly any observed level scheme. On the other hand, it may be noted that the j's describing the rotation levels are quite consistent, i.e., no non-integral numbers have been used. Furthermore, the j values repeat between successive vibration (n) levels.

While Wilson's theory does not predict the existence of levels, the calculation may lead to a more

exacting search for an apparently missing level when a particular j value within a vibration band is absent. For example, the observed resonance at 12.07 Mev may be compared about equally well with a calculated level for $n = 30$, $j = 6$ or 7. The discrepancy between observed and calculated levels for either value of j is larger than at any other place in the table. Reference to Fig. 8-3 shows that the observed resonance at 12.07 Mev (generating voltmeter = 62.5) is rather broader than the others, and suggests that a more exacting investigation might resolve this peak into two, such that both $j = 6$ and $j = 7$ will be more nearly satisfied.

The Gamma Ray Yield

The gamma ray yield from a thin target of vanadium (17 kev) bombarded with protons, measured simultaneously with the neutron yield, is shown in Fig. 8-5. As before, the fractional standard deviation of each point is about 1 per cent. A comparison of Figs. 8-5 and 8-3 shows that for each peak of the gamma ray yield curve, there is a corresponding peak on the neutron yield curve, but the opposite is not true. Peaks of neutron yield for which there is no accompanying peak of gamma yield occur at 49.5, 57.5, and 58.5, corresponding to levels in the compound nucleus at 11.49, 11.84, and 11.89 Mev. The absence of these gamma peaks suggests that the above levels

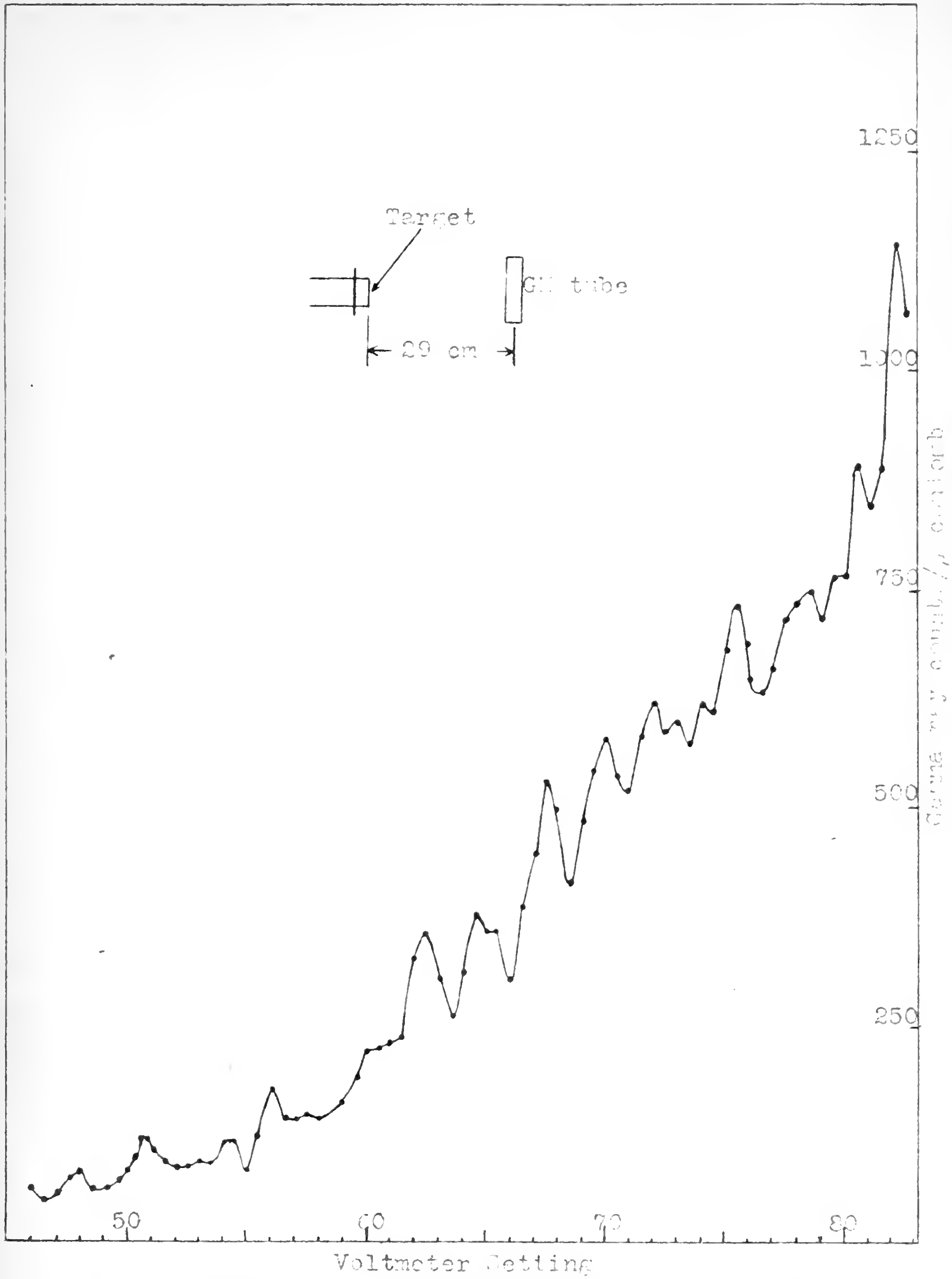

Fig. 8-5. Gamma ray yield from a thin (17 kev) vanadium target bombarded by protons.

of Cr^{52} decay to the ground state of Cr^{51}, while the other observed levels decay to excited states of Cr^{51}, which subsequently emits one or more gamma rays in transitions to the ground state.

Examination of Fig. 8-5 shows that the single peaks occurring at voltmeter settings of 56 and 62.5 on the neutron yield curve (Fig. 8-3) are here each resolved into two separate peaks. If, by further investigation, each of these peaks of the neutron curve can be resolved into two peaks, the absence of $j = 7$ for $n = 29$ will be explained. Furthermore, both $j = 6$ and $j = 7$ for $n = 30$, when substituted into Wilson's equation, will give calculated resonances agreeing with the observed levels, as has been discussed previously in connection with Table 8-2.

The $V^{51}(p,n)$ Cross Section, the Q Value, and the Cr^{51} - V^{51} Mass Difference

A rough estimate of the $V^{51}(p,n)$ cross section has been made by assuming the long counter to have nearly the same absolute sensitivity as the counter described by Hanson and McKibben. Thus one neutron count at 53 cm. represents a source strength of 1.7×10^4 neutrons. Referring to Fig. 8-2, the counting rate is ~ one neutron per μ coulomb at 50 kev above threshold for a V target 2000 Å thick. The cross section is then roughly:

$$\sigma = \frac{\text{neutrons}/\mu\ \text{coulomb}}{(\text{protons}/\mu\ \text{coulomb})(\text{nuclei}/\text{cm}^3)(\text{thickness})}$$

$$\sigma = \frac{(1.7 \times 10^4)(1.6 \times 10^{-13})}{(.0704 \times 10^{24})(2000 \times 10^{-8})}$$

$$\approx 2 \times 10^{-3} \text{ barns.}$$

For heavy nuclei*, the Q value may be computed from

$$(E_p)_{\text{threshold}} = -\frac{M'}{M' - m_p} Q ,$$

where M' is the mass of the residual nucleus and m_p is the mass of the proton. Substituting the known values for the masses, the Q value is found to be -1.53 ± .02 Mev. This value for Q, when substituted into

$$V^{51} + H^1 \rightarrow n^1 + Cr^{51} + Q$$

gives the $Cr^{51} - V^{51}$ mass difference to be 0.00080 ± 0.00002 amu.

---

*For light nuclei, the Q value is found from the exact expression:

$$(E_p)_{th} = -Q \frac{M'}{M' - m_p + \frac{m_p\, m_n}{M' + m_n} \cos^2\theta}$$

CHAPTER IX

ENERGY LEVELS IN Ti^{46} AS DETERMINED FROM THE BOMBARDMENT OF Sc^{45} WITH PROTONS

Introduction

The reaction $\mathrm{Sc}^{45}(p,n)\mathrm{Ti}^{45}$ has been studied very little. Allen (Al 41) and his coworkers used the reaction to produce Ti^{45}, in order to measure the half-life of this nuclide. Hanson and Taschek (Ha 48) have measured the neutron yield from a thick scandium target for proton energies up to 3.5 Mev. We have confirmed Hanson and Taschek's results for thick targets. In addition, we have studied both the neutron and gamma-ray yield from a thin target for energies up to 3.74 Mev. The study of the scandium reaction is important for the same reasons as for vanadium, as discussed in the previous chapter. In addition, the neutron yield just above the threshold is some forty times as great in scandium as in vanadium (Ha 48).

It must be emphasized at the outset that the results described below should be considered as tentative. Lack of time has prevented a thorough verification of the yield curves obtained.

Thick Target Yield

A thick scandium target was prepared by evaporating a suspension of the oxide to dryness on a tantalum backing. The oxide sample used was prepared by Johnson, Matthey and Company, Limited, London, and was certified "spectrographically standardized".

The yield curve is plotted in Fig. 9-1. The threshold occurs at 2.90 ± 0.02 Mev proton energy. The probable error attributed to the measurement is a result of the uncertainty in beam energy. The break in the upper part of the curve corresponds to a similar break observed in the thin target yield upon which several resonances are superimposed.

Thin Target Yields

A thin scandium target was prepared by evaporation in vacuo, as described in Chapter V. The neutron and gamma-ray yields from this target are shown in Figs. 9-2 and 9-3 respectively. No attempt has been made to indicate the statistical error, since for most points the fractional standard deviation is less than 1%, except near threshold on the neutron yield curve where it rises to about 5%.

Using the same data which was used to construct the yield curves, the following table has been prepared:

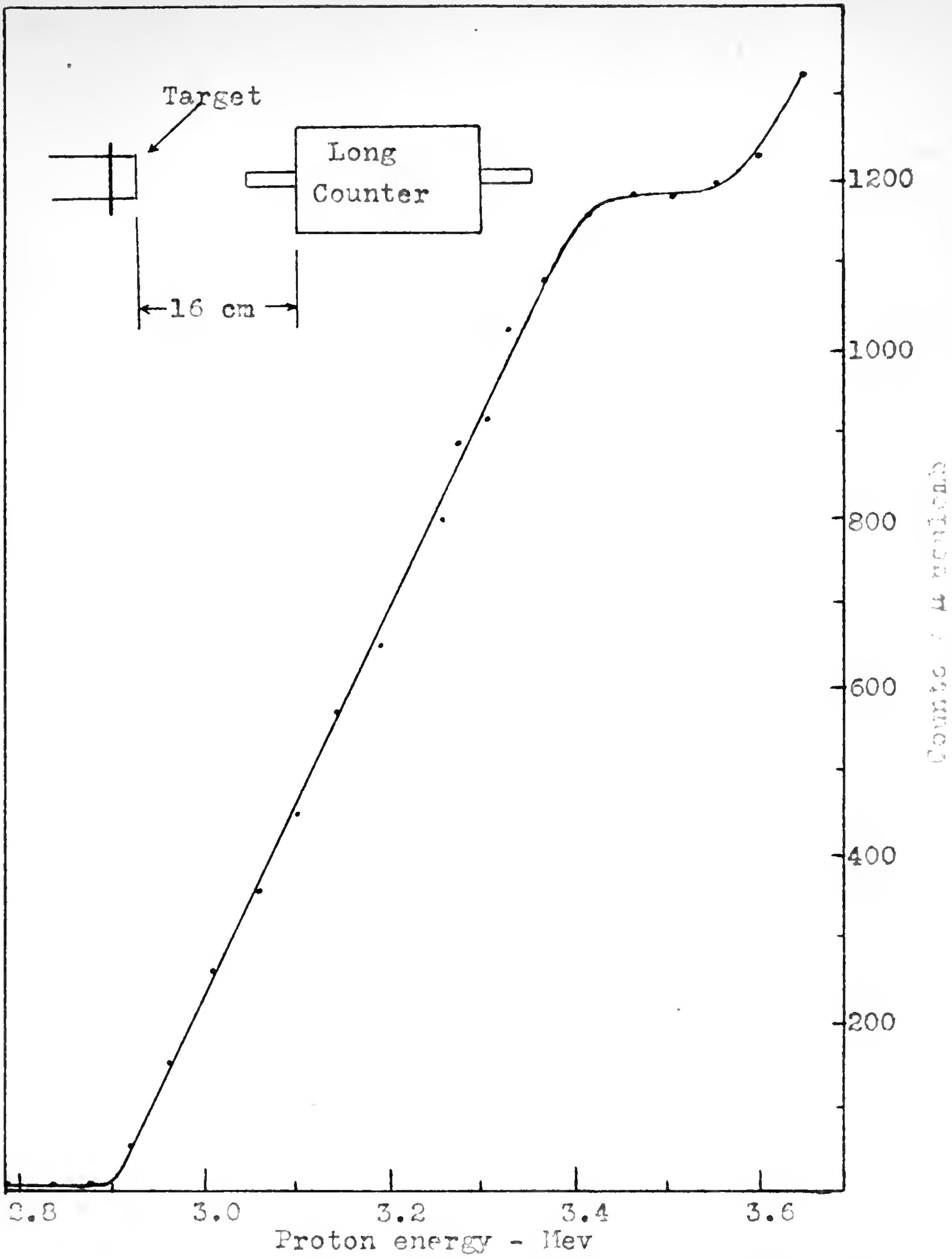

Fig. 9-1. Neutron yield from a thick scandium oxide target.

TABLE 9-1

Neutron Resonance	γ-Ray Resonance	$E(Ti^{46})$ Observed	E_{nj} Calculated	n	j
- -	1.40	9.66	9.688	24	7
- -	1.46	9.72	9.710	25	0
- -	1.50	9.76	9.749	25	2
- -	1.62	9.87	9.840	25	4
- -	1.72	9.97	9.984	25	6
- -	1.89	10.14	10.136	26	2
- -	1.94	10.19	10.175	26	3
- -	2.20	10.44	10.462	26	7
- -	2.34	10.58	10.562	27	3
- -	2.41	10.65	10.689	27	5
- -	2.54	10.77	10.758	27	6
- -	2.59	10.82	10.802	27	6 1/2
- -	2.63	10.86	10.849	27	7
- -	2.78	11.01	11.002	28	4
2.96	2.96	11.18	11.146	28	6
3.08	- -	11.30	11.299	29	2
3.12	3.12	11.34	11.368	29	3
3.17	3.17	11.39	11.390	29	4
- -	3.22	11.44	11.455	29	5
3.30	3.30	11.52	11.534	29	6
3.37	3.37	11.59	11.625	29	7
3.44	3.44	11.66	11.660	30	1
3.48	3.48	11.69	11.686	30	2
3.57	3.57	11.78	11.777	30	4
- -	3.64	11.85	11.835	30	5
- -	3.71	11.92	11.921	30	6

In this table, the first two columns represent proton energies in Mev corresponding to resonances observed in the yield curves. The values of $E(Ti^{46})$ are energy levels in Ti^{46} computed from

$$E(Ti^{46}) = (M_o + M_1 - M)c^2 + M_oE_1/(M_o + M_1)$$

where

M_o = mass of the Sc^{45} atom

M_1 = mass of the hydrogen atom

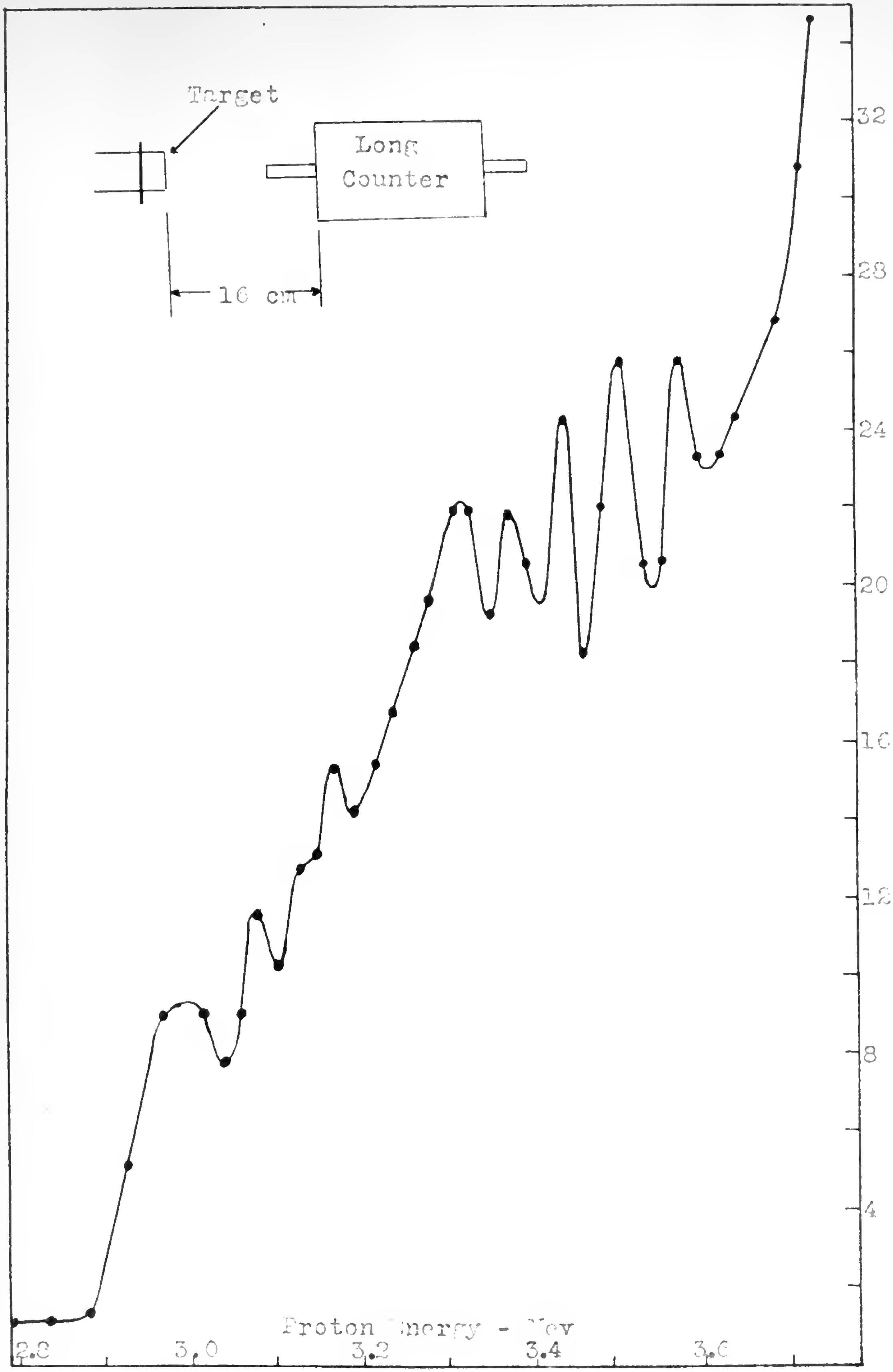

Fig. 9-2. Neutron yield from a twin Sc target.

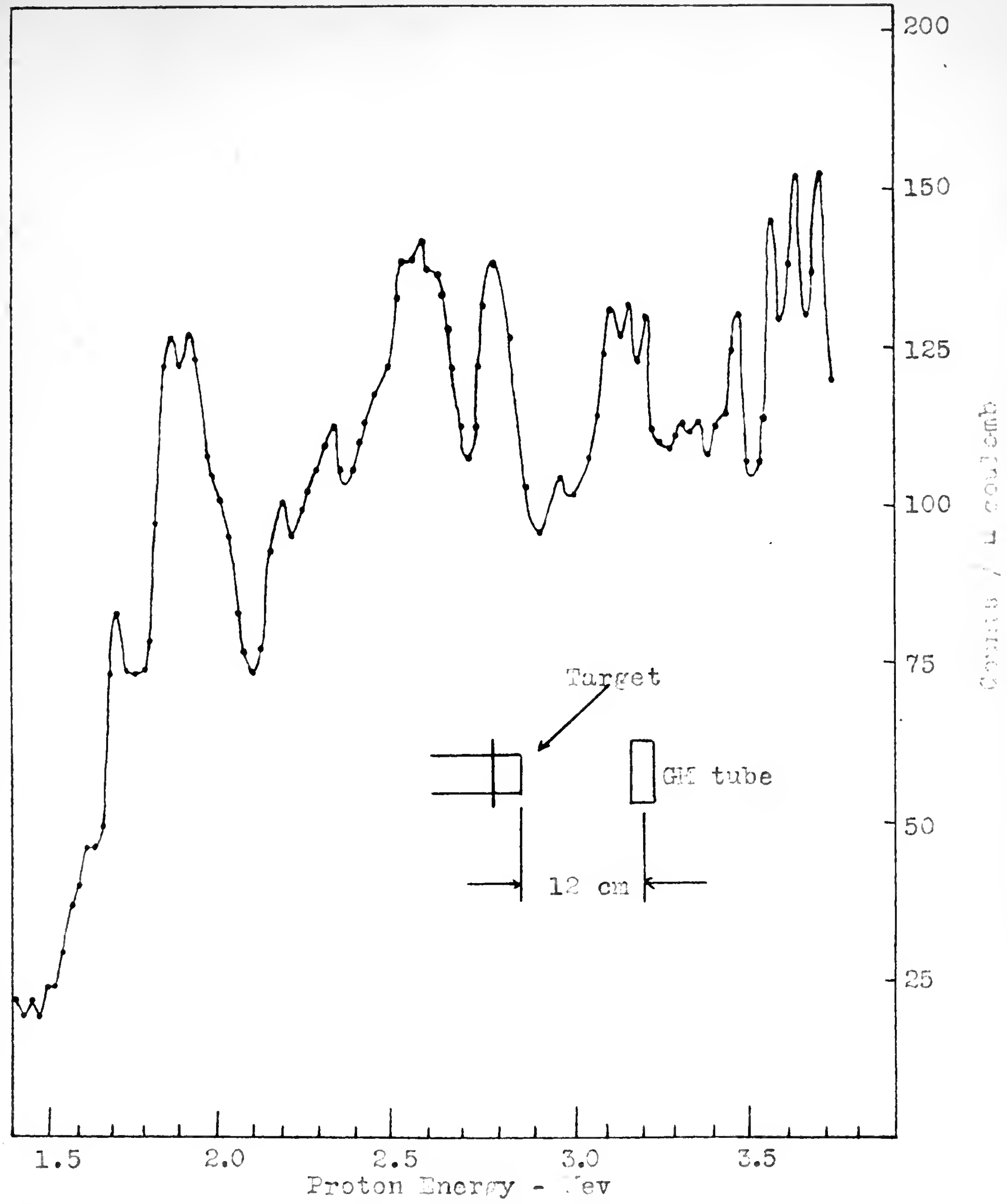

Fig. 9-3. Gamma ray yield from a thin Sc target.

M = mass of the Ti^{46} atom

E_1 = energy of the proton

c = velocity of light

The values of E_{nj} represent energy levels computed by the use of Wilson's formula (Wi 50),

$$E_{nj} = 0.387 \left[(n - 1)(n + 2)\right]^{1/2} + 1.44(AZ^4)^{-1/3}(j)(j + 1)$$

as was done for vanadium in the previous chapter. However, for scandium, the coefficient 0.387 was changed to 0.382 in order to arrive at the results shown in the table. The necessity for a correction of this nature could arise from the uncertainty in the mass differences used to compute the observed energy levels. The masses used were taken from Segre (1948), and the uncertainty is of the order of 100 kev, introducing the same uncertainty into the values of the observed energy levels.

The agreement between the observed and computed energy levels is not as good with scandium as with vanadium. By using slightly different values of the initial coefficient in Wilson's formula, and different n's and j's, other level schemes can be calculated which will fit the observed data about as well as the one proposed above. The one given is merely the best fit of several possibilities which were tried. The range of choice is so great that, as Wilson points out, "values of n and j

can be found to make the calculated values agree with the observed values within the limits of error in nearly all cases". Since the limits of error are large in this investigation, arising mainly from the uncertainty in mass differences, the comparison of observed and calculated values does not give a significant quantitative test of the theory.

The level spacings observed are of the order of 100 kev. Wilson suggests that this is about the spacing to be expected for all elements and all excitations, and that this spacing is from 1000 to 10,000 times greater than on other current theories for excitations of the order of 10 Mev. Qualitatively, then, the results obtained are in accord with Wilson's conclusions.

The data of Table 9-1 have been drawn into an energy level diagram, Fig. 9-4. Insufficient evidence is available to determine the mode of decay of the excited levels. A tentative transition to the ground state of Ti^{45} is indicated as possible on the basis of the two yield curves. This transition corresponds to a neutron resonance unaccompanied by a gamma-ray resonance.

The Q Value and the Ti^{45} - Sc^{45} Mass Difference

The Q value may be computed from

$$E_p \text{ (threshold)} = - \frac{M'}{M' - m_p} Q$$

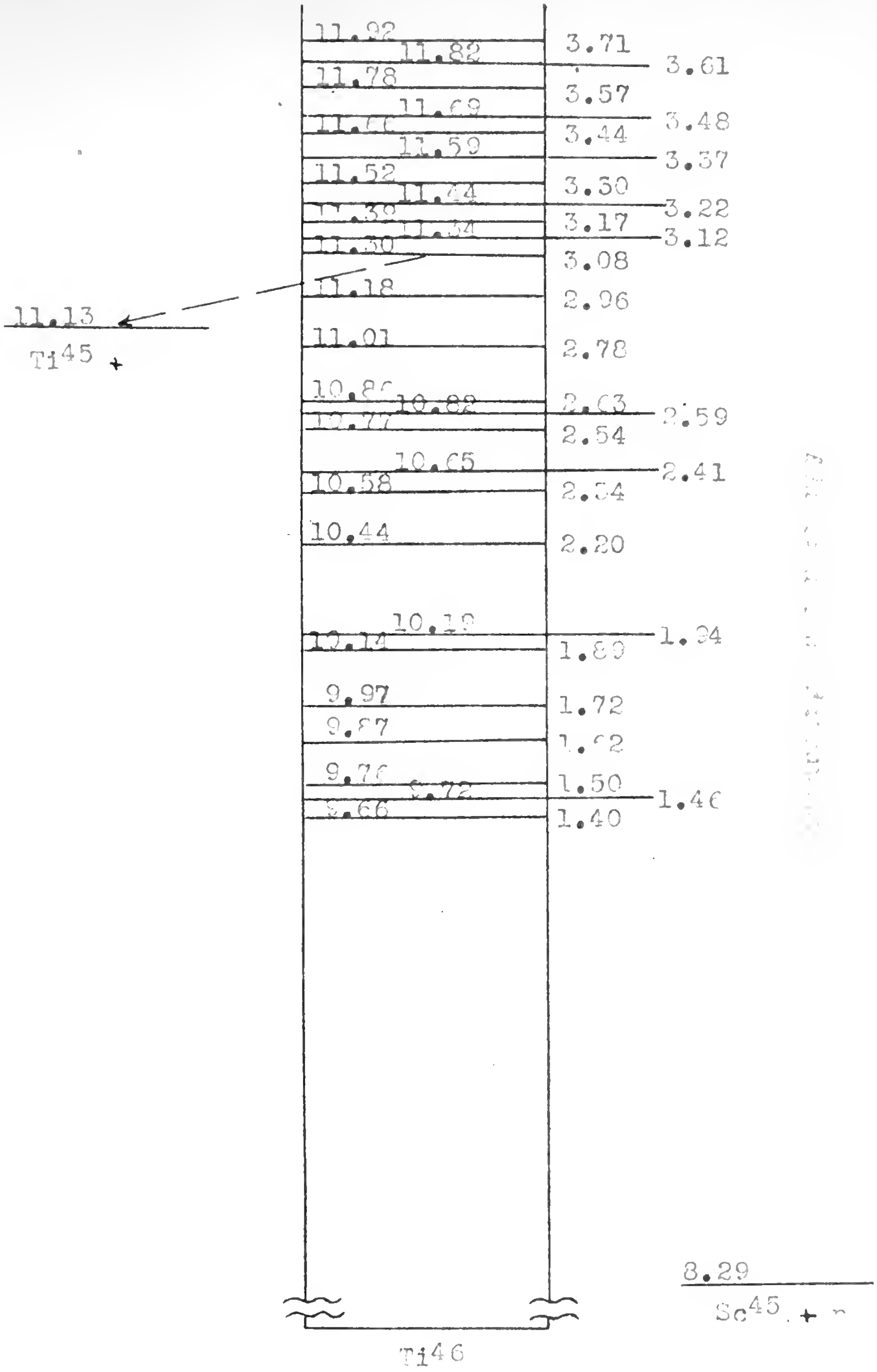

Fig. 3-4. Tentative energy level diagram for Ti^{46}. Only levels found in this investigation are shown.

where M' is the mass of the residual nucleus and m_p is the mass of the proton. Substituting the known values, the Q value is found to be -2.84 ± 0.02 Mev. Substituting this value of Q into

$$\mathrm{Sc}^{45} + \mathrm{H}^{1} \longrightarrow \mathrm{Ti}^{45} + \mathrm{n}^{1} + \mathrm{Q}$$

gives 0.00220 = 0.00002 amu for the Ti^{45} - Sc^{45} mass difference. Therefore, to the accuracy of the Sc^{45} mass given in Segre (1948), the mass of Ti^{45} is 44.9691 amu.

CHAPTER X

SUGGESTIONS FOR FURTHER INVESTIGATION

The installation of the magnetic resonance beam energy control will permit an energy resolution of nearly 0.01 per cent to be secured at the Rockefeller Generator. The installation of equipotential shells should permit bombarding energies of almost 5 Mev to be reached. With these two improvements in the generator, the investigations reported in Chapters VII, VIII, and IX of this paper can profitably be repeated, with the view in mind of establishing the location of additional excited states in the nuclei of Be^8, Ti^{46}, and Cr^{52}, at energies higher than presently attainable.

Efforts should be made to determine the modes of de-excitation of the levels reported, for example, by measuring the energy of the gamma rays associated with a particular level. Such investigations will be difficult and extensive in the case of Ti^{46} and Cr^{52} since the levels are so numerous and closely spaced. The knowledge of modes of decay would be valuable in assigning values of angular momentum and parity (possibly) to the various states. Sufficient information of this nature will even-

tually lead to a more exact understanding of selection rules governing nuclear transitions.

Two of the levels in Be^8 require immediate attention. The first of these, at 18.36 Mev above the ground state, should be investigated to prove conclusively whether the level belongs to Be^8 or one of the target impurities listed in Chapter VII. Secondly, the energy of the gamma rays associated with the level at 19.23 Mev should be determined. If this energy turns out to be about 0.4 Mev, then the gamma rays almost certainly result from the decay of an excited state of Be^7. This measurement will do much to resolve the doubt now extant concerning the existence of a level in Be^7 at $\sim$ 0.4 Mev. If such a level can be shown to exist, then it follows at once that Li^7 loses its value as a monoenergetic neutron source for proton bombarding energies greater than 2.31 Mev. Unfortunately, the neutron and gamma ray intensities from a Li target at this bombarding energy are too low to permit coincidence techniques to be used. One will probably have to be satisfied with a simple absorption experiment to determine the gamma ray energy.

It would be desirable to try to fit Wilson's spherical shell model to as many nuclei as possible. If the same formula for excited states can be shown, however empirically, to fit all nuclei, or all nuclei within a given region of mass number, then the very fitting of the formula to a series of observed levels in a nucleus will

enable one to obtain the target nucleus - compound nucleus mass difference accurate to 0.00001 amu. The method for making this determination has been indicated in Chapters VII and IX under the discussion of the applicability of Wilson's model to Be^8 and Ti^{46}.

During the course of the investigations described in previous chapters, a parallel plate proportional counter was constructed in which it was planned to place various elements for study under neutron bombardment. This counter was made from one originally designed as a fission counter (Servo Lab Dwg. 6546CN035). It was modified by removal of pieces 5 and 9 and substituting therefor a high voltage connection with teflon insulation. The anode plate was removed and replaced with a nickel ring 6.2 cm. in diameter on which a grid of 0.5 mil wolfram wire spaced at 1 cm. was spot welded. The brass cathode plates on either side of the anode are easily removed for coating with the desired element. The counter is provided with valves for operation as a flow counter. Using an $A-CO_2$ (5%) mixture as flow gas, the counter was successfully operated with hydrogen recoils (cathodes coated with wax) and with the $B^{10}(n,\alpha)Li^7$ reaction (cathodes coated with B_2O_3).

Insufficient time was available to perform the desired experiments with the counter. However, it is felt that it may advantageously be used with the coincidence circuit of Chapter II for the investigation of en-

ergy levels in nuclei, by coating the cathodes with an element which produces a charged particle accompanied by a gamma ray when bombarded by neutrons. The scintillation counter described in Chapter II would be used to detect the gamma ray, and energy measurements on the gamma ray could be made readily by inserting absorber between the two counters.

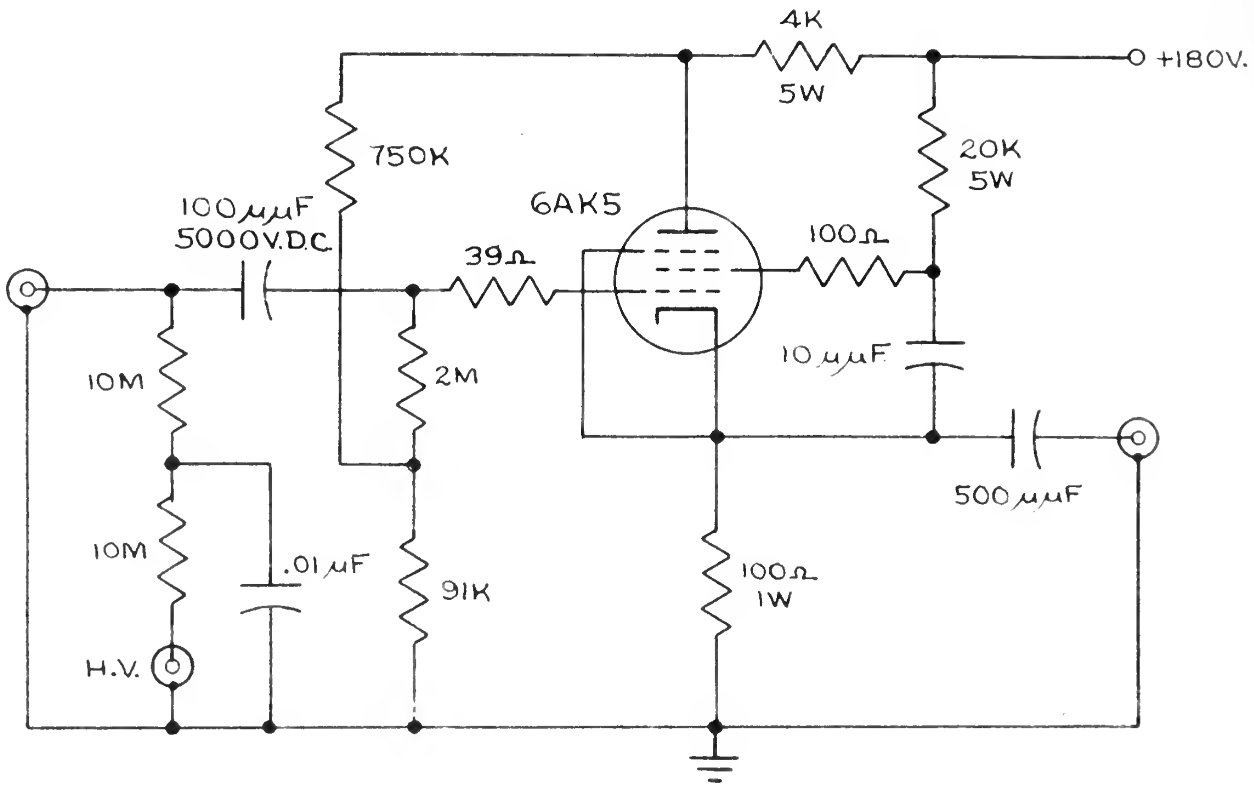

FIG. A-1 BF_3 COUNTER PREAMPLIFIER

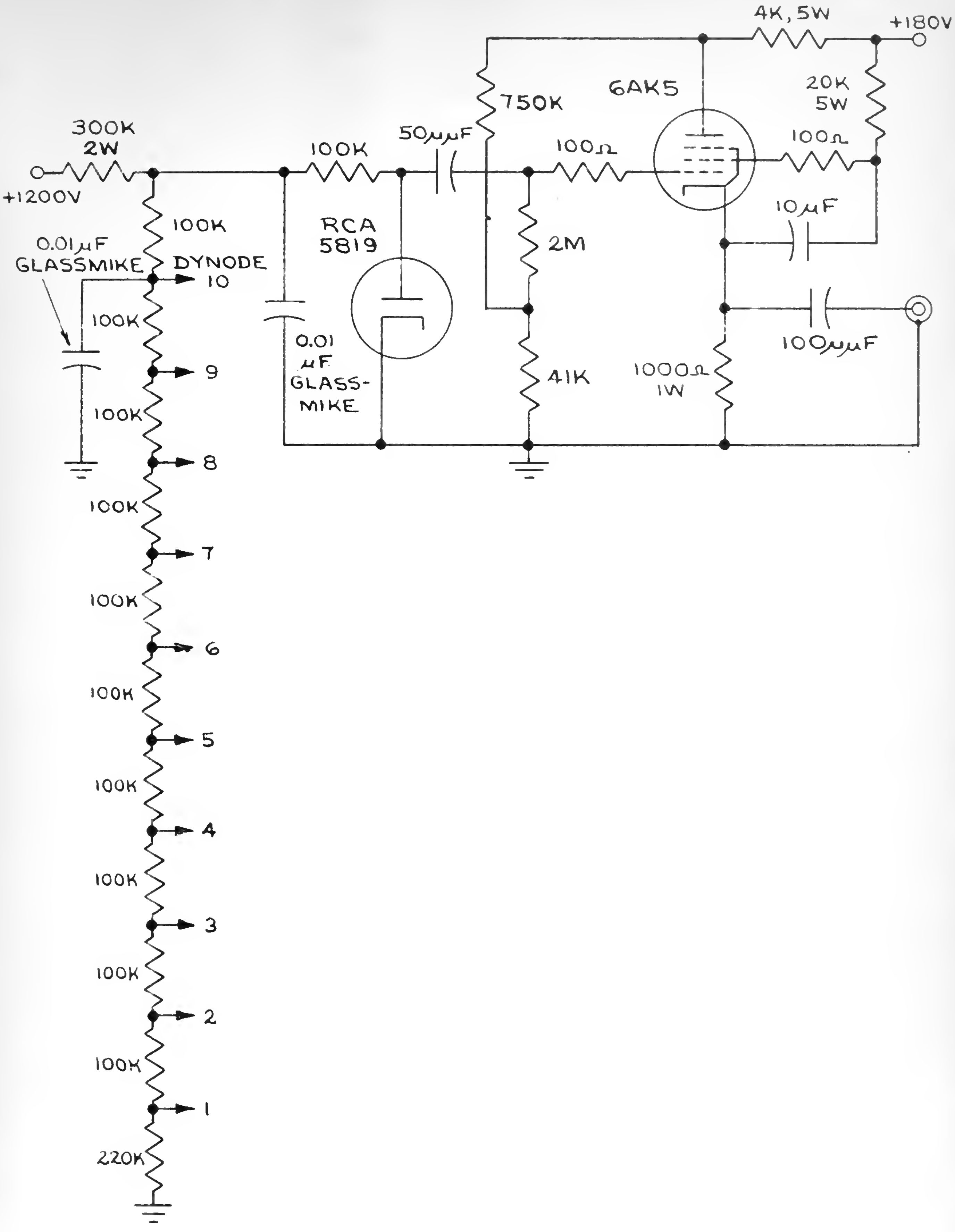

FIG A-2 SCINTILLATION COUNTER PREAMPLIFIER

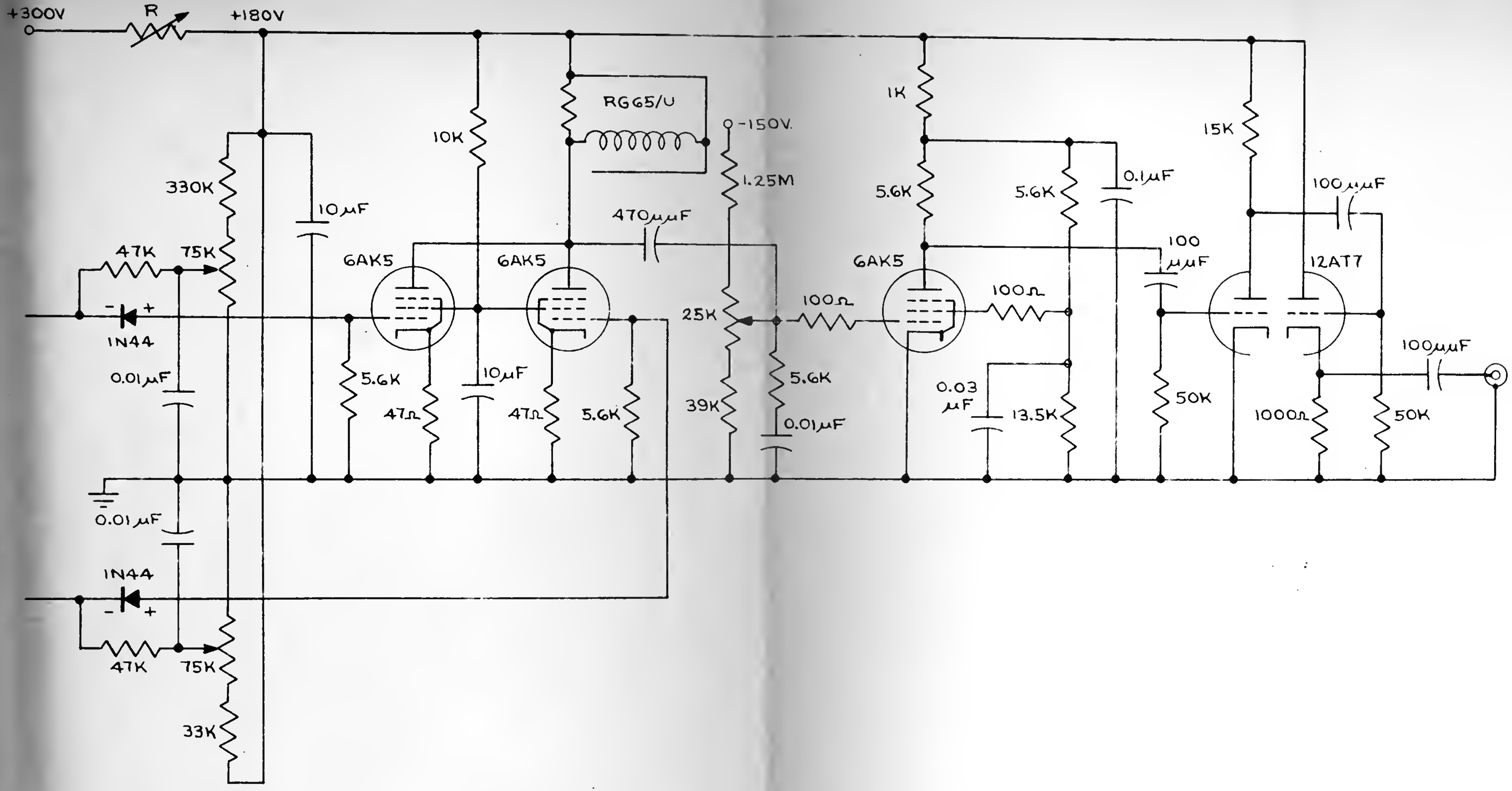

FIG. A-4 COINCIDENCE CIRCUIT

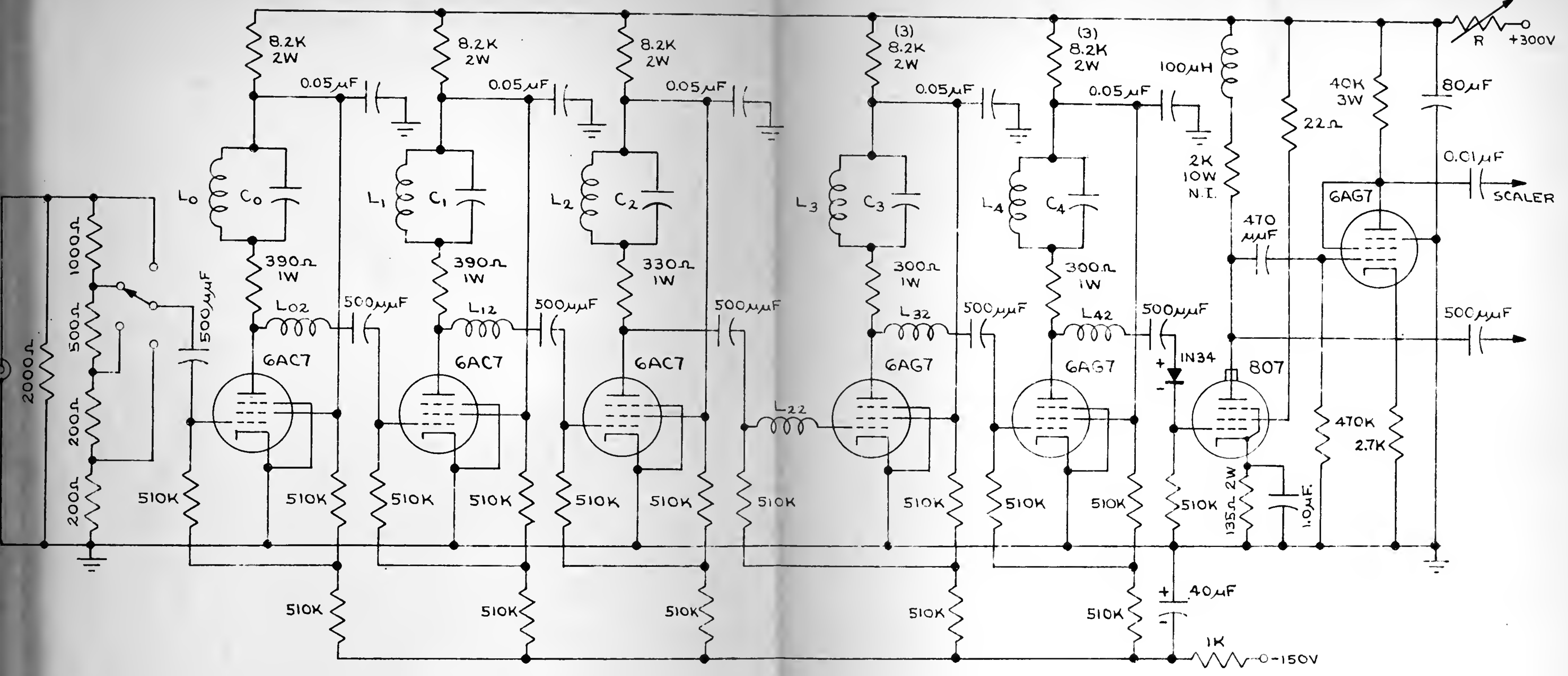

FIG. A-3 FAST PULSE AMPLIFIER

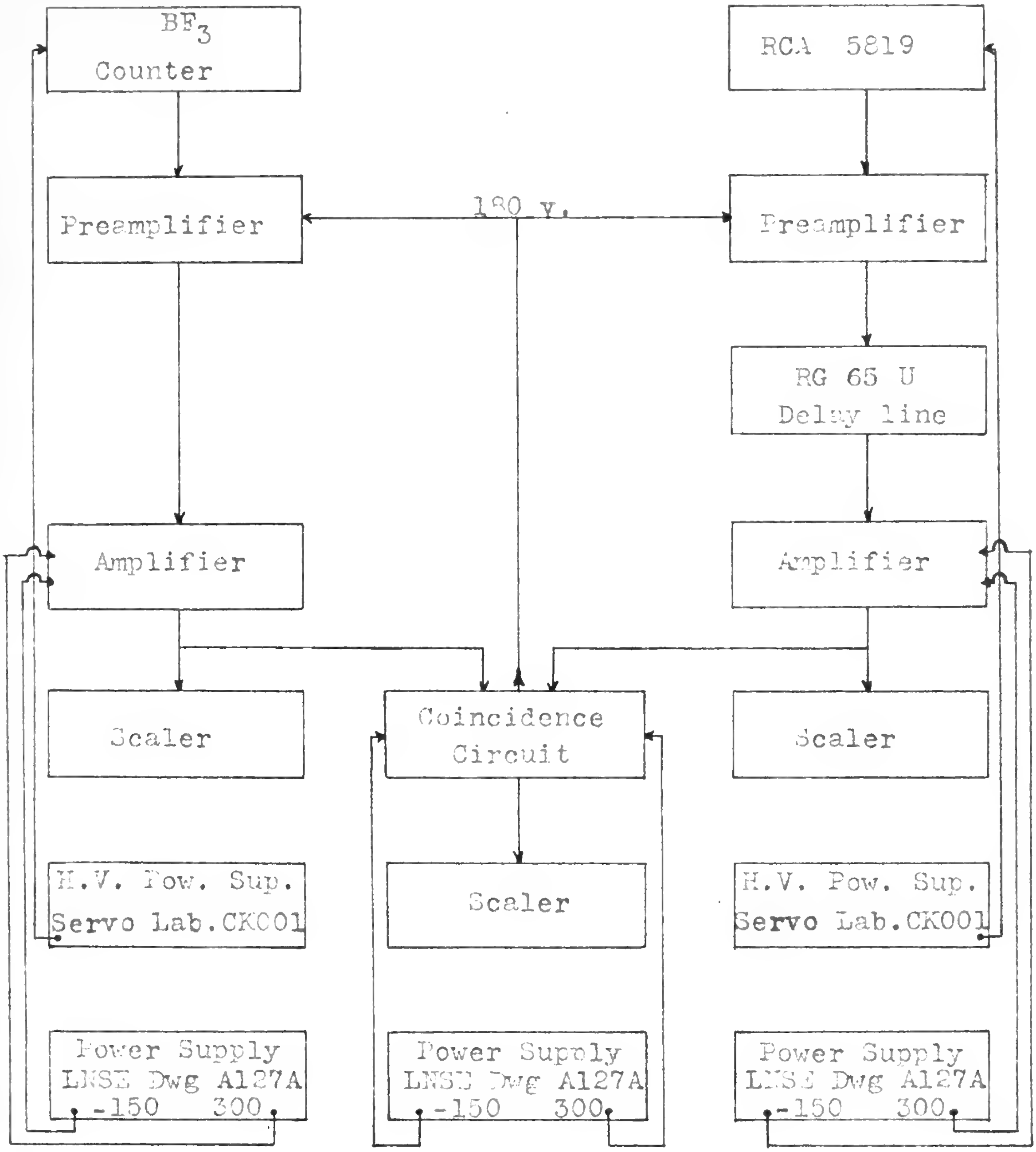

Fig. A-5. Block diagram of the complete coincidence counting system.

APPENDIX II

BIBLIOGRAPHY

Al 41 Allen, J.S.V., et al., PR 60, 425 (1941).

Be 49 Bell, P.R., private communication.

Bj 38 Bjerge, T., Proc. Roy. Soc. 164, 243 (1938).

Bl 46 Bloch, F., PR 70, 460 (1946).

Bl 46a Bloch, F., et al., PR 69, 127L (1946).

Bl 46b Bloch, F., PR 70, 474 (1946).

Br 45 Bradt, H., et al., Helv. Phys. Act. 18, 259 (1945).

Bu 49 Buechner, W.W., and Strait, E.N., PR 76, 1547 (1949).

Co 48 Collins, G., PR 74, 1543(L) (1948).

Da 48 Dare, J.A., and Rowen, W.H., Lab. for Nuc. Sci. and Eng. Technical Report No. 6, M.I.T., 1948.

Da 49 Dacey, J.E., and Paine, R.W., Jr., Nuclear Shielding Studies III, "Shielding Properties of Various Materials Against Neutrons and Gamma Rays," M.S. Thesis, M.I.T., January 1949.

De 45 Demers, P., Montreal Laboratory Reports MP-74 and MP-204.

De 47 Deutsch, M., PR 72, 729 (1947).

Du 40 Dunworth, J.V., RSI 11, 167 (1940).

El 48 Elmore, W.C., Nucleonics 2, No. 3, 16 (1948).

El 48a Elmore, W.C., Nucleonics 2, No. 2, 4 (1948).
Ibid., Nucleonics 5, No. 3, 48 (1949).
Ibid., J. App. Phys. 19, 55 (1948).

Em 49 Engineering Memoranda, Electronics Nuclear Instrumentation Project, D.I.C. 6663, M.I.T. See Memoranda Nos. 6, 13, and 16.

Ev 48 Evans, R.D., and Evans, R.O., RMP 20, 305 (1948).

Ga 49 Garlick, G., and Fateholly, R., PR *75*, 1290A (1949).

Gr 40 Graves, E.R., PR *57*, 855 (1940).

Gr 49 Graves, E.R., *et al.*, RSI *20*, 579 (1949).

Gr 50 Grosskreutz, J.C., and Mather, K.B., PR *77*, 580 (1950).

Ha 47 Hanson, A.O., and McKibben, J.L., PR *72*, 673 (1947).

Ha 48 Hanson, A.O., and Taschek, R.F., National Research Council *Preliminary Report No. 4*, "Monoenergetic Neutrons from Charged Particle Reactions."

He 49 Hess, D.C., *et al.*, PR *76*, 1717 (1949).

Hl 48 Hornyak, W.F., and Lauritsen, T., RMP *20*, 191 (1948).

Ho 47 *Handbook of Chemistry and Physics*, 30th Ed., Chemical Rubber Co., Cleveland, Ohio, 1947.

Ho 48 Hofstadter, R., PR *74*, 100 (1948).

Ho 49 Hofstadter, R., *et al.*, PR *75*, 1290A (1949).

Jo 49 Jordan, W.H., and Bell, P.R., Nucleonics *5*, No. 4 (1949).

Jo 50 Johnson, Laubenstein, and Richards (to be published in PR).

La 50 Lauritsen, T., and Thomas, R.G. (to be published in PR).

Le 44 Leverenz, H.W., Proc. I.R.E., *32*, 256 (1944).

Ma 49 Mattauch, J., and Flammersfeld, A., "Isotopic Report," Verlag der Zeitschrift fur Naturforschung (1949).

Mo 48 Moon, R.J., PR *73*, 1210 (1948).

Nu 49 Nuclear Shielding Group Minutes, M.I.T., January 25, 1949.

Ob 34 O'Bryan, H.M., RSI *5*, 125 (1934).

Or 49 Oak Ridge National Laboratory, ORNL *366*, *Quarterly*

Progress Report 15, June 1945.

Ow 44 Owen-Harries, J.H., Electronics, Sept. 1944.

Pe -- Perlman, I.H., Richards, H.T., and Speck, L., MDDC-39.

Ra 79 Lord Rayleigh, Proc. Roy. Soc. Lond., XXIX, 71 (1879).

Ra 46 Rainwater, J., and Havens, W.W., PR 70, 136 (1946).

Ro 47 Rossi, B.B., and Staub, H.K., Ionization Chambers and Counters, McGraw-Hill Book Co., Inc., New York, 1947.

Ro 48 Rose, B., Can. Jour. Res., A26, 366 (1948).

Sh 49 Shoupp, W.E., et al., PR 76, 502 (1949).

Si 46 Siegbahn, K., Arkiv. Mat. Ast. Fysik, B 34, No. 6 (1946).

Si 47 Siegbahn, K., and Slatis, H., Arkiv. Mat. Ast. Fysik, A 34, No. 15 (1947).

Sm 48 Smith, R.V., and Richards, H.T., PR 74, 1257 (1948).

Sm 50 Smith, R.V., and Richards, H.T., PR 77, 752 (1950).

Ta 49 Taschek, R.F., PR 75, 1361 (1949).

Tl 49 Tollestrup, A.V., et al., PR 76, 428 (1949).

To 49 Torrey, H.C., PR 76, 1059 (1949).

Wd 50 Willard, H., currently working with the Li^7(p,n) reaction at M.I.T.

Wi 41 Wison, R.S., Proc. Roy. Soc. Lond., A177, 382 (1940-41).

Wi 50 Wilson, H.A., PR 77, 516 (1950).

Ya 46 Yalow, A.A., et al., PR 69, 253A (1946).

Zl 42 Zlotowski, I., and Wiliams, J., PR 62, 29 (1942).